

Spatial modeling of the highest daily maximum temperature in Korea via max-stable processes

Youngsaeng Lee, Sanghoon Yoon, Md. Sharwar Murshed

Dept of Statistics, Chonnam National University, Gwangju, Korea

Maeng-Ki Kim

Dept of Atmospheric Sciences, Kongju National University, Gongju, Korea

Chun-Ho Cho, Hee-Jeong Baek

Climate Research Division, National Inst of Meteorological Research, Seoul, Korea

Jeong-Soo Park**

Dept of Statistics, Chonnam National University, Gwangju, Korea

Abstract

This paper examines the annual highest of daily maximum temperature in Korea by using data from 56 weather stations and employing a spatial extreme modeling. Our approach is based on the max-stable processes with Schlather's characterization. We divide the country into four regions for a better model fit and identify the best model for each region. Comparing the maps of predicted return levels for ungauged sites are computed by three different methods. We demonstrate the superiority (based on the experts' eye view) of max-stable process modeling over a generalized extreme value model and Kriging. A cluster analysis by using geographic variables and return levels is presented. The advantage of the spatial extreme modeling approach is that it can be used to consider problems concerning aggregation of the max-stable processes over the country and the interpolation to anywhere within the region. Thus, more precise return levels and some indices of the highest temperatures can be obtained for locations with no observed data, and help to determine the effects and vulnerability assessments of extreme events at the local level.

Keywords: Cluster analysis, Composite likelihood, Daily maximum temperature, Extremal coefficient, Generalized extreme value distribution, Kriging, Max-stable processes, Multivariate extremes, Return level, Spatial extremes.

*Technical Report, Dept of Statistics, Chonnam National University, Korea (Second revised at September 28, 2012). Available at <http://stat.jnu.ac.kr/bbs/zbxe/?mid=introPJS>

**Corresponding author (Email: jspark@jnu.ac.kr)

1. Introduction

Increases in extreme climatic events, such as prolonged periods of hot days and intense heavy rainfall days, have greater negative impacts on human society and natural environments than changes in climatic means (*Choi et al.*, 2009). In Korea, for example, above-average temperatures continued for 81 days during summer and last until the middle of September 2010. This means that the number of heat wave days is 28% higher than the average (*Korea Meteorological Administration (KMA)*, 2010). The more the global mean temperature changes, the more likely the extreme events are and their consequent effects on organisms and ecosystem (*USCCP*, 2008; *Hongmei et al.*, 2009). Unfortunately, because extreme events occur at different spatial scales such that climate observations are limited and geographic conditions vary widely, any spatial modeling of the annual highest daily maximum temperature (DMT) should be conducted a high confidence level.

Statistical inferences involve drawing conclusions based on data and prior assumptions. For a spatial data analysis, a key insight is that observations in space cannot typically be assumed to be mutually independent and that those observations that are close to each other are likely to be similar. This insight has been applied to the modeling of spatial extreme events, which have received increasing attention in recent years. This spatial modeling of extreme values takes spatial dependence and extreme properties into account simultaneously to obtain return levels and some indices for locations with no observed data. This study's modeling is based on the max-stable processes (MSP). We employ Schlather's characterization of the MSP to draw statistical inferences about the spatial extreme data.

Univariate extreme value theory is well known as a statistical technique for modeling extreme data (*Kotz and Nadarajah*, 1999; *Coles*, 2001; *Beirlant et al.*, 2004; *Resnick*, 2007). Generalized extreme value (GEV) and generalized Pareto distributions are widely used to model extreme values. Extreme value distributions are typically employed independently for each weather station. In this regard, the better approach for avoiding local fluctuations may be to build a model for the whole set of stations.

Although models for multivariate extreme values are less widely used in practice, a number of studies have provided diverse statistical theories (for example, *de Haan and Resnick* (1977); *de Haan* (1985); *Coles and Tawn* (1991)). Previous studies of multivariate extremes typically consider a small number of variables (e.g., 2 or 3). Many environmental phenomena, however, have a spatial dimension, and thus, the objective is to model the spatial dependence within extreme events in continuous space based on recorded observations for a grid (*Beirlant et al.*, 2004). Several studies suggest some methods for addressing spatial extremes, for example, *Smith* (1990); *Schlather and Tawn* (2003); *Buishand et al.* (2008); *Davison* (2009); *Sang and Gelfand* (2010). Such methods are generally based on the max-stable processes (*de Haan*, 1984), a stochastic process in which all finite-dimensional distributions are multivariate extreme value distributions. In terms of asymptotic motivation, the max-stable processes can be regarded as a spatial analogue of the univariate GEV distribution. Thus, the max-stable processes may be an appropriate technique for modeling spatial extreme data. Recently, *Blanchet and Davison* (2011) and *Davison and Gholamrezaee* (2012) applied the max-stable process to extreme snow

depth and annual maximum temperature in Switzerland, respectively.

Table 1: Each station's code and name, sample statistics including minimum of annual highest daily maximum temperature (DMT), sample median, IQR (interquartile range), sample L-skewness and maximum of annual highest DMT for 15 selected stations (unit: degree Celsius), where statistics are calculated from 37 years of data (1973-2009) for all stations.

Site	Name	Min	Median	IQR	L-skew	Max
101	Chuncheon	32.9	35.2	1.5	-0.2092	36.5
105	Gangneung	31.8	36.0	1.7	-0.0892	39.3
108	Seoul	31.6	35.0	1.7	-0.1693	38.4
112	Incheon	29.5	33.6	1.6	-0.0790	37.2
114	Wonju	31.5	34.8	1.2	-0.1038	38.0
133	Daejeon	32.2	34.4	1.5	0.0268	37.7
135	Chupungyeong	30.8	34.1	1.9	-0.0432	36.8
140	Gunsan	30.5	34.3	1.2	-0.2156	36.9
143	Daegu	33.9	36.5	2.2	0.0776	39.5
156	Gwangju	31.7	35.0	1.2	-0.0995	38.5
159	Busan	30.7	33.0	1.7	0.0512	36.7
165	Mokpo	29.5	34.0	1.6	-0.1543	37.0
168	Yeosu	29.4	32.8	2.1	0.0488	37.1
170	Wando	28.9	32.8	1.7	-0.0203	36.3
289	Sancheong	32.1	35.7	1.8	-0.0032	39.3

This paper examines the annual highest DMT from 1973 to 2009 for 56 weather stations in Korea by using a spatial extreme model. We obtained the data from the Korea Meteorological Administration (<http://www.kma.go.kr>). Table 1 present the code/name and sample statistics for each of the 15 selected stations. Figure 1 shows the histograms of the highest DMT for 6 selected stations for a general overview of the distribution. We select only 6 stations to show the three typical distributions (left-skewed, symmetric, and right-skewed).

We first construct a MSP model for entire region (over South Korea) to analyze the data. However, because the model does not provide a good fit to the data for some cities, we divide the country into four regions: the northwestern, northeastern, southwestern, and southeastern regions (Figure 2). We then achieve a better fit and identify the best model for each region. We present the estimates of various parameters and their standard errors, return levels for several return periods, and contour maps based on the return levels. Comparing the maps of predicted return levels for ungauged sites (computed using three different methods), we demonstrate the superiority (based on the experts' eye view) of MSP modeling over the GEV model and Kriging. The advantage of the spatial extreme modeling approach is that it can be used to consider problems concerning the aggregation of the global process over the country and the interpolation to anywhere within the region. Thus, more precise return levels and some indices of the highest DMT can be obtained for locations with no observed data.

The rest of this paper is organized as follows: Section 2 provides a brief review of previous research on the MSP modeling of extreme values. Section 3 presents the results for the MSP

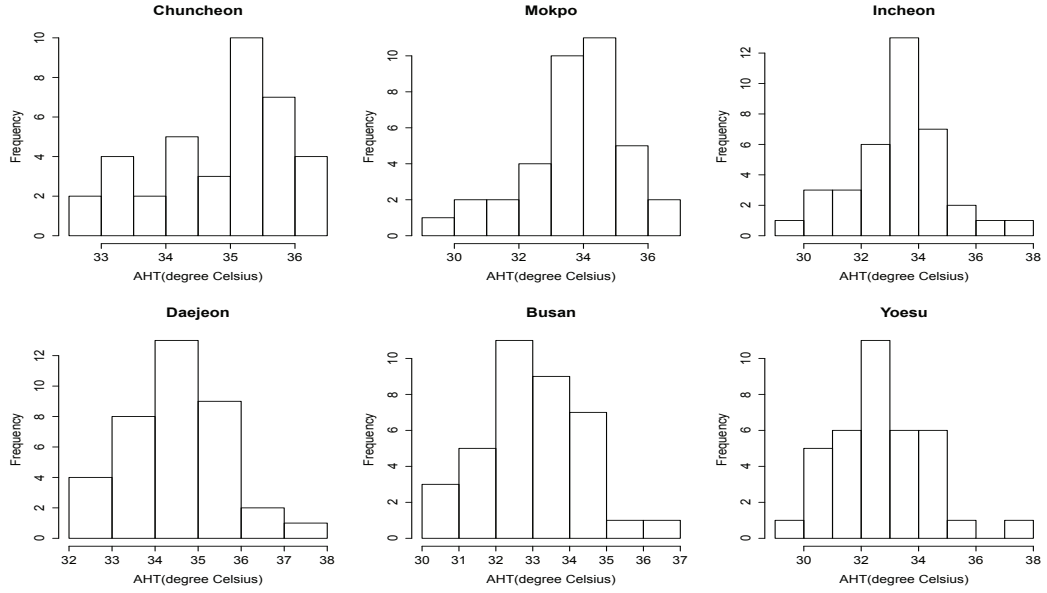


Figure 1: Histograms of the annual highest temperature for six selected stations representing three typical (left-skewed, symmetric and right-skewed) distributions.

model, and Section 4 concludes. This study is motivated by *Davison* (2009) and *Gholamrezaee* (2009), and some descriptions of the MSP in this paper are excerpted from *Westra and Sisson* (2011). For the analysis, we intensively used *SpatialExtremes*, an R package developed by *Ribatet* (2009).

2. Spatial modeling of extreme values

2.1. Univariate extreme distribution

The generalized extreme value (GEV) distribution, which is as flexible as the three well-known extreme value distributions (i.e., Gumbel, Fréchet and negative Weibull), is widely used for the analyzing univariate extreme values. The cumulative distribution function (CDF) of the GEV distribution is as follows:

$$G(x) = \exp \left\{ - \left(1 + \xi \frac{x - \mu}{\sigma} \right)^{-1/\xi} \right\}, \quad 1 + \xi(x - \mu)/\sigma > 0, \quad (1)$$

where μ , σ and ξ are the location, scale, and shape parameters, respectively. The particular case of (1) for $\xi = 0$ is the Gumbel distribution, whereas the cases for $\xi > 0$ and $\xi < 0$ are known as the Fréchet and negative Weibull distributions, respectively (*Kotz and Nadarajah*, 1999; *Coles*, 2001). Extreme value distributions are typically applied independently for a set of weather stations. However, a better approach may be to build a model for the whole set of weather stations to avoid local fluctuations and reflect the fact that many environmental processes have a spatial domain.

For understanding MSP, we may need the definition of max-stability (*Coles*, 2001).

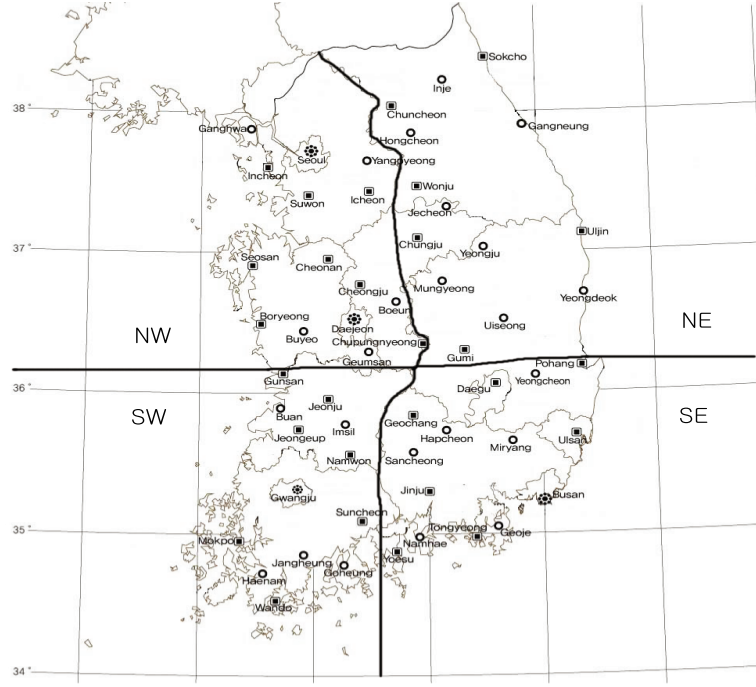


Figure 2: Map of South Korea with 56 weather stations, and four regions: northwestern (NW), southwestern (SW), northeastern (NE), southeastern (SE).

Definition (max-stability): A distribution G is said to be max-stable if, for every $n = 2, 3, \dots$, there are constants $\alpha_n > 0$ and β_n such that

$$G^n(\alpha_n z + \beta_n) = G(z).$$

In the course of analysis of spatial extremes, models for multivariate extremes are considered.

2.2. Multivariate extremes

Applications of multivariate extreme value theory include a wide range of problems in which there are several variables or processes being studied (*Zhang and Smith, 2010*). In general, maxima or minima are defined “componentwise” across a sequence of random vectors in multivariate extreme value theory. Following *Hüsler* (2009), we briefly discuss a bivariate case with independent and identically distributed (iid) random vectors (X_{1i}, X_{2i}) , $i = 1, \dots, n$, for simplicity. For a suitable normalization a_n , b_n , c_n and d_n with positive a_n , c_n :

$$\begin{aligned} & P\left\{ \left(\max_{i \leq n} X_{1i} - b_n \right)/a_n \leq x_1, \left(\max_{i \leq n} X_{2i} - d_n \right)/c_n \leq x_2 \right\} \\ &= F^n(a_n x_1 + b_n, c_n x_2 + d_n) \rightarrow G(x_1, x_2) \end{aligned}$$

as $n \rightarrow \infty$, where $F(x_1, x_2)$ denotes the bivariate distribution of (X_{1i}, X_{2i}) and $G(x_1, x_2)$ is the limiting bivariate extreme value distribution. If F is such that (2) holds, then $G(x_1, x_2)$ satisfies a bivariate version of the max-stability property, which defines a class of multivariate extreme

value distributions, as in the univariate case. Each marginal distribution has to be one of the univariate GEV distributions. One standard class for bivariate extremes is the logistic family: $G(x_1, x_2) = \exp\{-(x_1^{-1/\alpha} + x_2^{-1/\alpha})^\alpha\}$, $x_1 > 0$, $x_2 > 0$, for the parameter $\alpha \in (0, 1)$. This distribution possesses a bivariate version of the property of max-stability. For more details, see *Beirlant et al.* (2004) and *Resnick* (2007).

2.3. Max-stable processes

The Max-stable process (MSP) is an infinite-dimensional generalization of multivariate extreme value distributions and is particularly applicable in the context of a time series or a spatial process. The theory of MSP, introduced by *de Haan* (1984), has been studied by a number of researchers, for example *Smith* (1990); *Coles* (1993); *Schlather* (2002); *de Haan and Lin* (2003); *de Haan and Pereira* (2006).

The MSP $Z(\cdot)$ is defined as the limit process of maxima of independent and identically distributed random fields $Y_i(x)$, $x \in R^d$ and can be expressed as (*de Haan*, 1984)

$$Z(x) = \lim_{n \rightarrow \infty} \frac{\max_{i \leq n} Y_i(x) - b_n(x)}{a_n(x)}, \quad (2)$$

if the limit exists for all x in R^d with normalizing constants $a_n(x) > 0$ and $b_n(x) \in R$. The MSP is a direct extension of the univariate GEV model to the spatial domain. Max-stable processes are the limits of pointwise maxima processes in the same way that the GEV family is the limit distribution of block maxima, and the bivariate extreme value family is the limit distribution of componewise block maxima (*Coles*, 2001). According to *de Haan and Resnick* (1977), for a fixed point (x) in space, any d-dimensional marginal distribution belongs to a class of multivariate extreme value distributions. In practice, this means that the resulting parameters $\mu(x)$, $\sigma(x) > 0$, and $\xi(x)$ are the continuous functions to be estimated. Thus the MSP naturally permits modelling and predictions with data-level spatial dependence (*Westra and Sisson*, 2011).

Given a series of n observations at K spatial locations, the aim of a statistical analysis would be to fit a MSP using assumed forms for the parameters $\mu(x)$, $\sigma(x)$, and $\xi(x)$, while also estimating spatial dependence. However, for more than $K = 2$ spatial locations, the distribution function of the general MSP has no analytically tractable form, which thereby presents a problem for practical statistical model fitting, and so ad hoc characterization methods have been proposed (*Westra and Sisson*, 2011).

There are several characterizations of the MSP. *Smith* (1990) introduced the first method, and more recently, *Schlather* (2002) introduced another method. *Davison* (2009) and *Kabluchko et al.* (2009) considered other Gaussian process models that turn out to be the same as the Smith model except for the parameter $a(h)^2$ in the next equation (3) (*Padoan et al.*, 2010). *Coles* (1993) provided a class of MSP models that can make use of all data exceeding a predefined threshold. MSP is used by *Coles and Walshaw* (1994) to model the directional dependence of extreme wind speeds.

Considering exactly $K = 2$ spatial locations (e.g., x_1 and x_2), *Smith* (1990) uses the normal probability density and derives a bivariate CDF as

$$-\log \Pr \{Z(x_1) < z_1, Z(x_2) < z_2\}$$

$$= \frac{1}{z_1} \Phi \left\{ \frac{a(h)}{2} + \frac{1}{a(h)} \log \left(\frac{z_2}{z_1} \right) \right\} + \frac{1}{z_2} \Phi \left\{ \frac{a(h)}{2} + \frac{1}{a(h)} \log \left(\frac{z_1}{z_2} \right) \right\} \quad (3)$$

for the MSP $Z(x)$, where $h = (x_1 - x_2)$ is the distance vector between locations x_1 and x_2 , and $a(h) = (h^t \Sigma^{-1} h)^{1/2}$,

$$\Sigma = \begin{bmatrix} \sigma_{11} & \sigma_{12} \\ \sigma_{12} & \sigma_{22} \end{bmatrix} \text{ or } \Sigma = \begin{bmatrix} \sigma_{11} & \sigma_{12} & \sigma_{13} \\ \sigma_{12} & \sigma_{22} & \sigma_{23} \\ \sigma_{13} & \sigma_{23} & \sigma_{33} \end{bmatrix}, \text{ and so forth.} \quad (4)$$

Here Φ is the standard normal distribution function, $a(h)$ is the weighted distance between x_1 and x_2 , and Σ is the (unknown) covariance matrix representing spatial dependence.

Schlather's characterization involves a correlation function $\rho(x)$. He derives a bivariate CDF as

$$V(z_1, z_2) = -\log \Pr \{Z(x_1) \leq z_1, Z(x_2) \leq z_2\} = \frac{1}{2} \left(\frac{1}{z_1} + \frac{1}{z_2} \right) \times \left\{ 1 + \sqrt{1 - 2(\rho(h) + 1) \frac{z_1 z_2}{(z_1 + z_2)^2}} \right\}, \quad (5)$$

where h is the distance between x_1 and x_2 . Further, $\rho \in [0, 1]$, where the lower bound corresponds to the independence of extremes. In this paper, we use Schlather's characterization, in which $\rho(h)$ is a powered exponential covariance function of distance h (Cressie and Wikle, 2011), to adjust the spatial model

$$\rho(h) = \nu \exp \left\{ - \left(\frac{h}{\tau} \right)^\eta \right\}, \quad 0 < \eta \leq 2, \quad \tau > 0, \quad 0 \leq \nu \leq 1, \quad h > 0, \quad (6)$$

where τ and η are the scale and shape parameters respectively. The parameter ν represents the nugget effect of measurement errors and microscale variations in the data. If $\nu = 0$, then the whole process is a nugget process, and if $\nu = 1$, then there is no nugget process. Large τ reflects high correlations between nearby observations, whereas small τ reflects low correlations. The shape parameter η is related to the smoothness of the observation surface. The case $\eta = 2$ gives an infinitely differentiable (smooth) surface. Small η gives a non-differentiable surface with a tendency to return to the grand mean over the spatial region.

In the above two characterizations, a MSP $Z(x)$ has a marginal unit Fréchet distribution, that is, $\Pr(X_i < z) = \exp(-1/z)$, $z > 0$ for a marginal random variable X_i . This is a special case of the GEV distribution with parameters $\mu = 0$, $\sigma = 1$, and $\xi = 1$. However, observations are not drawn from a unit Fréchet distribution, and thus, we rewrite them for unknown GEV margins. We can define the transformation such that

$$t : Z(x) \mapsto \left(1 + \xi(x) \frac{Z(x) - \mu(x)}{\sigma(x)} \right)^{1/\xi(x)} \quad (7)$$

where $Z(\cdot)$ is a max-stable random field having GEV margins with parameters $\mu(x)$, $\sigma(x)$, $\xi(x)$ (Padoan et al., 2010).

2.4. Composite likelihood and estimation

Because finding higher-order distribution functions for the MSP is difficult, we employ the composite likelihood estimation method to construct a likelihood-like object by using the bivariate density function from (5). The idea behind this method is to use lower-order density functions such as bivariate functions.

Following *Gholamrezaee* (2009), suppose that X is a d -variate random variable with the density function $f_X(\cdot; \theta)$. If X_1, \dots, X_n are independent copies of X , then the composite likelihood (CL) function of order $r = 1, \dots, d$ equals

$$CL_r(\theta) = \prod_{k=1}^n \prod_{i_1 < \dots < i_r} f_X(x_{i_1}^{(k)}, \dots, x_{i_r}^{(k)}; \theta), \quad (8)$$

where $i_j \in \{1, \dots, d\}$ for $j \in \{1, \dots, r\}$, and $x_{i_j}^{(k)}$ is the k -th observation of the i_j -th site. The full likelihood is a special case of the CL for $r = d$. For example, if $r = 2$, then $CL_2(\theta)$ is referred to as a pairwise likelihood function. We use this pairwise likelihood function because only the bivariate density function is specified for the MSP.

Subject to suitable regularity conditions (*Padoan et al.*, 2010), the maximum pairwise likelihood estimate provides consistent and unbiased parameter estimates and confidence intervals. Let ψ be the parameters to be estimated, including ν , τ , η in (6) and coefficients in the regression-based forms for $\mu(x)$, $\sigma(x)$, $\xi(x)$. It is known that (*Ribatet*, 2009)

$$\hat{\psi}_p \sim N(\psi, H(\psi)^{-1} J(\psi) H(\psi)^{-1}), \quad n \rightarrow \infty, \quad (9)$$

where $\hat{\psi}$ is the maximum pairwise likelihood estimator of ψ , $J(\psi) = \text{Var}[\nabla l_p(\psi; Y)]$, and $H(\psi) = E[\nabla^2 l_p(\psi; Y)]$. Therefore, the usual suite of statistical techniques are available, resulting in a powerful and flexible inferential framework. It is then trivial to build regression-based forms for the parameters $\mu(x)$, $\sigma(x)$, $\xi(x)$ and estimate spatial dependence parameters (*Westra and Sisson*, 2011).

The use of the pairwise likelihood method leads to an under-specified model (*Ribatet*, 2009). Thus, the Akaike information criterion (AIC) is not appropriate for the CL method. Instead, we use the Takeuchi information criterion (TIC) to select a better model (*Varin and Vidoni*, 2005). The model with a low TIC is the good one:

$$TIC = -2l_p(\hat{\psi}; y) - 2 \text{tr}(J(\hat{\psi})H(\hat{\psi})^{-1}), \quad (10)$$

where $J(\hat{\psi}) = J(\psi)|_{\psi=\hat{\psi}}$, $H(\hat{\psi}) = H(\psi)|_{\psi=\hat{\psi}}$, and $l_p(\hat{\psi}; y)$ are the pairwise likelihood value at $\psi = \hat{\psi}$. *Ribatet* (2009) provides the computational details of estimating $J(\hat{\psi})$ and $H(\hat{\psi})$.

3. Data and modeling

3.1. Data and climate

In this study, we use daily maximum temperature (DMT) data from 56 weather stations (except for Jeju Island) for the 1973-2009 period (see Figure 2). We exclude one station (Daegwanryong) because the behavior of the station differs significantly from that of others. In Korea, the best conditions for the annual highest temperature are found in August because weather conditions are favorable to high insolation after the rainy season from late June to July. For most weather stations, the observed daily maximum temperature mainly occurs during the afternoon, whereas the observed daily minimum temperature occurs mainly during the early hours of the morning (*Hopkinson et al.*, 2011). Previous studies (e.g., *Easterling et al.* (1997); *Caesar et al.* (2006)) have demonstrated that increasing trends in the daily minimum temperature exceed

those in the DMT for most regions, indicating a diurnal temperature range (DTR). *Robinson et al.* (1995) used daily maximum and minimum temperatures to derive climatic parameters such as the length of the growing season, heating/cooling degree days, and the variability of the annual temperature cycle.

In summer (July and August), a high pressure system known as the subtropical high develops over the North Pacific Ocean. This monsoon system makes westerly and southwesterly flows in Korea more pronounced. In addition, the development and northward extension of the North Pacific subtropical high play an important role in having synoptic environments in Korea to show the highest DMT (e.g., the inflow of warm air, clear skies, and increased solar radiation to the surface).

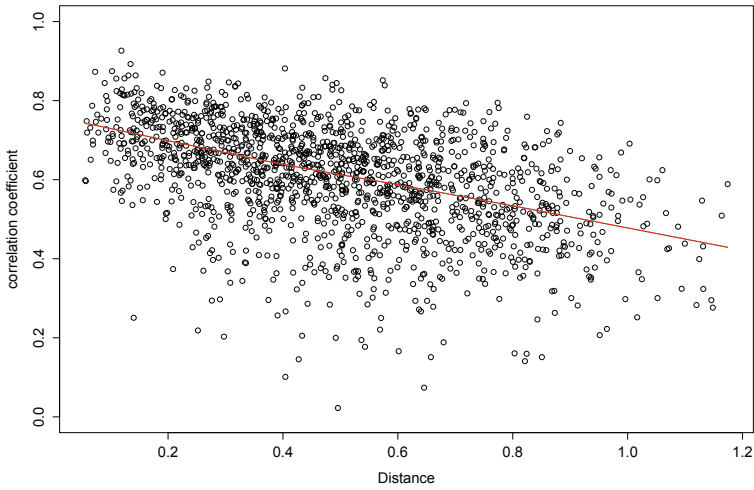


Figure 3: Scatter plot of Spearman correlation coefficients versus Euclidian distances obtained between every two stations.

Table 1 shows the maximum value of the annual highest DMT over 39 degrees Celsius for Daegu, Sancheong, and Gangneung, which are located on the eastward slope of the Sobaek and Taebaek Mountains, respectively. Daegu and Sancheong are located in basins, indicating that the rain shadow effect occurs frequently and it is easy to accumulate heat in a basin. The maximum value for Gangneung is mainly due to the fohn induced by the westerly flow over the Taebaek Mountains. A minimum value less than 30 degrees Celsius is found for islands and coastal areas such as Wando, Yeosu, Mokpo, and Incheon because it is easy to diffuse heat by a natural ventilation effect and cooler sea surface temperature. However, as shown in Figure 1, the histograms of the annual highest DMT are more complex than the sample statistics in Table 1. In fact, the histograms for each station cannot be classified into the three typical distributions (left-skewed, symmetric, and right-skewed), indicating that the shape of a distribution may be associated with the station's costal proximity, elevation, latitude, and longitude. This means that spatial modeling has to be considered as a function of these parameters.

For the data analysis, we employ the following linear transformation to make the station's

geographical information be in $[0, 1]$:

$$x_{new} = [x - \text{Min}(x)]/[\text{Max}(x) - \text{Min}(x)]. \quad (11)$$

This makes the calculation of the inverse of the Hessian matrix $H(\psi)$ more stable. According to the data, the minimum and maximum values of latitudes, longitudes, and altitudes are (34.23, 38.15) degrees, (126.22, 129.24) degrees, and (1.3, 263.1) meters, respectively.

Figure 3 provides a scatter plot of Spearman correlation coefficients versus Euclidian distances (obtained between every two stations in the sample). There is moderate spatial dependence for the highest daily temperature, suggesting that spatial modeling might be better than independent modeling.

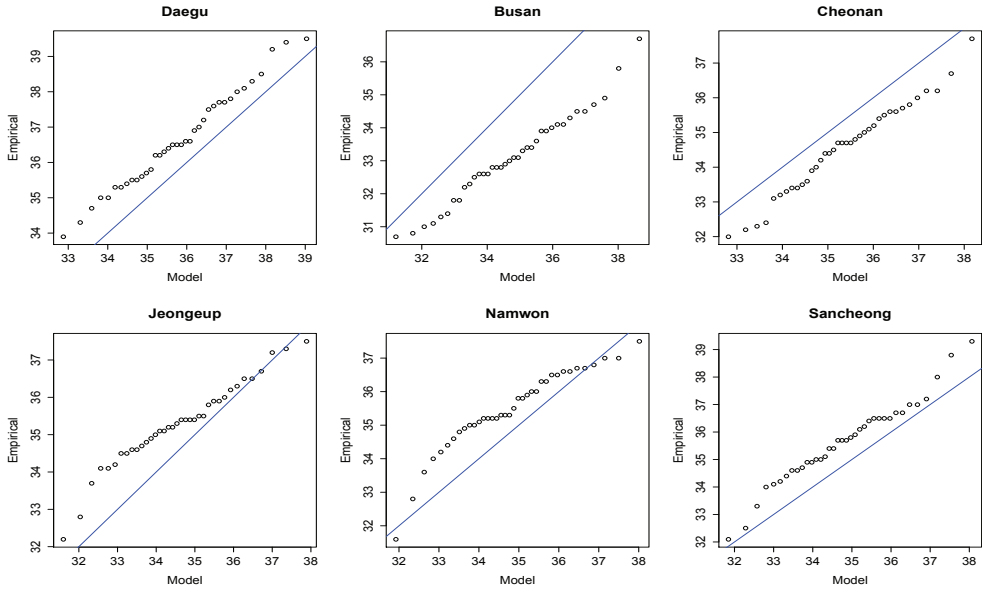


Figure 4: Quantile per quantile plots of six stations with the worst fits for the entire region model (unit: degrees Celsius).

3.2. Model fitting over the entire region

We fit the univariate GEV model to the temperature data for each station. The results indicate that the location parameter generally has a linear and quadratic relationship with the latitude and a linear relationship with the altitude and the longitude (not shown here). After some trials, we add the covariates “coast” and “city” to take the distance to coast and the urbanization effect into account, respectively. Thus, we build a regression-based form to the location parameter $\mu(x)$ by including these variables, where x denotes the station, $\text{coast}(x)$ is a categorized value (from 1 to 6) based on the distance to the nearest coast, and $\text{city}(x) = 1$ if the city’s population in the year 1990 is greater than or equal to one million and 0 otherwise. In this paper, we treat $\xi(x)$ as a constant ξ . For the scale parameter $\sigma(x)$, we construct a regression-based form. Through a model selection procedure, we obtain the following model which has the smallest TIC:

$$\sigma(x) = \sigma_0 + \sigma_{lat} \text{lat}(x) + \sigma_{lat^2} \text{lat}(x)^2 + \sigma_{coast} \text{coast}(x). \quad (12)$$

Table 2: Estimated parameters and standard errors in parenthesis for four regional models (n: the number of sites).

Parameters		NorthWest (n=15)	NorthEast (n=14)	SouthWest (n=13)	SouthEast (n=14)
$\rho(h)$	ν	0.74(0.07)	0.88(0.10)	0.81(0.04)	0.69(0.07)
	τ	0.80(0.25)	0.23(0.08)	0.59(0.14)	0.91(0.26)
	μ_0	37.40(0.66)	30.34(0.96)	32.27(0.29)	32.25(0.36)
	lat	-13.99(2.01)	10.67(2.41)	14.75(1.07)	17.99(1.56)
	lat^2	10.62(1.63)	-7.35(1.60)	-29.21(2.20)	-12.36(2.51)
$\mu(x)$	lon			5.31(0.22)	
	lon^2		0.94(0.22)		-1.81(0.22)
	alt	-0.006(0.0004)	-0.007(0.001)	-0.008(0.0005)	-0.008(0.0006)
	$coast$	-0.86(0.03)	0.22(0.05)		
$\sigma(x)$	σ_0	1.23(0.12)	1.61(0.13)	1.76(0.14)	2.05(0.23)
	lat	0.42(0.12)		-1.23(0.18)	-1.61(0.45)
	alt				-0.0007(0.0003)
	$coast$	-0.03(0.01)	-0.06(0.01)		0.04(0.02)
ξ	ξ	-0.24(0.05)	-0.29(0.05)	-0.26(0.06)	-0.298(0.05)

We do not report the estimates of the parameters and their standard errors for this model because it does not provide a good fit to the data. Noteworthy is that, based on the model selection procedure, we no longer include the "city" covariate in the location and scale parameter functions (even for the next regional models). This can be explained by the findings of *DeGae-tano and Allen* (2002) and *Karl et al.* (1993), who suggest that the maximum temperature is less likely to be affected by urbanization than the minimum temperature. Figure 4 shows the quantile-quantile (qq) plots for the worst 6 stations, which show the model is not satisfactory. The reason why the model does not provide a good fit to the data for some cities may be because we used only one model to the entire region. Thus, for a better model fit, we divided the country into four regions by considering the number of stations, administrative information, and geographical proximity (see Figure 2).

3.3. Regional modeling and diagnostics

For the four regions (i.e., northwestern(NW), northeastern(NE), southwestern(SW), and southeastern(SE)), we select the best model for each region by using the TIC. Here we fix $\eta = 1.5$ following *Gholamrezaee* (2009) and *Davison* (2009). Table 2 shows the estimates of various parameters and their standard errors. One may be concerned about sample size problem in estimating a total of 43 parameters for 56 stations. However, this may not be a serious problem because we consider a total of 2,072 ($=37 \times 56$) observations. The estimates of ν indicate weak nugget effects for four regions. The estimates of τ show moderately high dependence between observations from neighboring stations for the NW and SE regions but low dependence for the NE region. All estimates far exceed their standard errors, indicating a low probability of over-fitting. Further, the negative values of the shape parameter ξ for all four regions generally indicate a short tail for the distribution of the annual highest DMT.

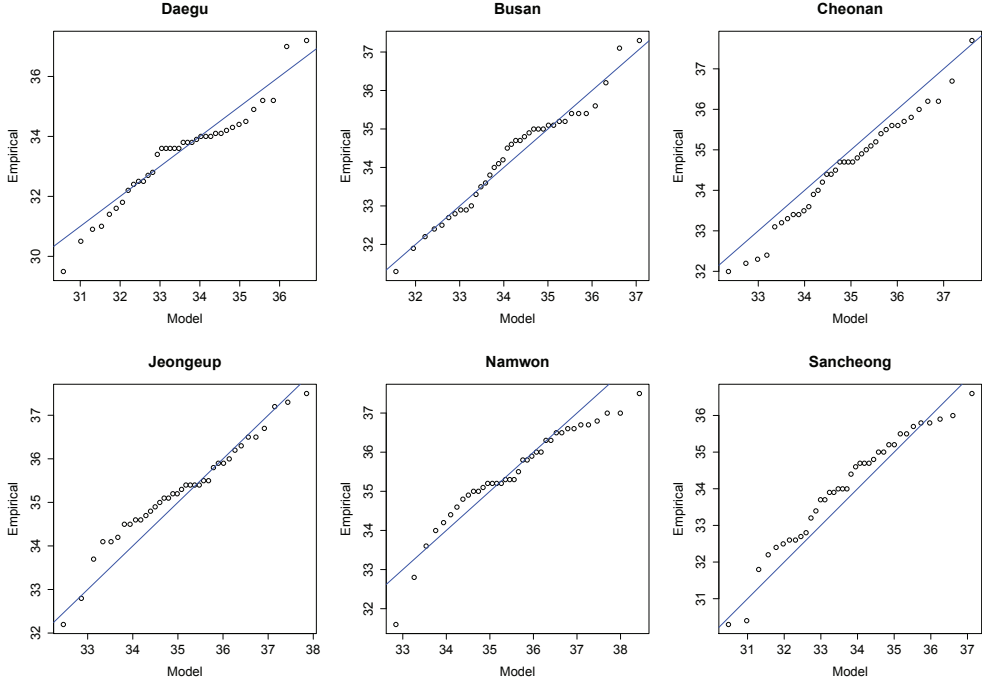


Figure 5: Quantile per quantile plots obtained from the four regional models for the same six stations which were considered in Figure 4 (unit: degrees Celsius).

As shown in Table 2, some covariates are included for modeling $\mu(x)$ and $\sigma(x)$ for each region. For $\mu(x)$, latitude, the square of latitude, and the altitude are included for all four models, whereas the longitude and the coastal area are included for some models. For $\sigma(x)$, the longitude has no influence, and the altitude has some influence only for the southeastern region. For selecting these covariates among many possible regression-based forms, we first set σ to be a constant. Then, from all possible forms of $\mu(x)$, we select combination of covariates at the minimum of TIC. Further, by fixing those covariates in $\mu(x)$, we select the best combination of covariates for $\sigma(x)$ that minimizes the TIC.

Table 3: Pearson correlation coefficients of parameters μ and σ estimated using the maximum likelihood estimation method from independent GEV distributions and from the max-stable process model for the entire region and for four subregions.

Region	$\text{corr}(\hat{\mu})$	$\text{corr}(\hat{\sigma})$
Entire	.755	.442
NW	.929	.693
NE	.676	.515
SW	.946	.758
SE	.946	.477

Figure 5 shows the q-q plots obtained by using the regional models for the stations considered in Figure 4. As shown in Figures 4 and 5, the regional models provide a substantially better

fit to the data than the country model.

Figure 6 shows the scatter plots for the parameters μ and σ estimated using the MLE method from independent GEV distributions (vertical axis) and from the MSP model (horizontal axis) for the four regions. Table 3 shows the Pearson correlation coefficients between these estimates for each parameter. High correlations for $\hat{\mu}$ and moderate correlations for $\hat{\sigma}$ for the four regional models and the improvement over the country model (except for the northeastern region) indicate that the regional MSP models are better. The estimates of σ from the southwestern and southeastern regions exceed those of σ from independent (or local) GEV models for most stations (see Figure 6). This provides evidence that the MSP model can account for many observations from neighboring stations instead of using observations from only one site. Another reason for this result may be due to the setting of the shape parameter $\xi(x)$ as a constant across regions because the estimates of σ and ξ are correlated. That is, the under-specifying ξ of the MSP model may make the estimate of σ biased and larger.

As another diagnostic tool for MSP modeling, a q-q plot based on comparing groupwise maxima observed from data with values simulated from the fitted MSP model can be useful (Davison, 2009). Figure 7 shows the q-q plots for the four regions at the 95% confidence level, which indicate that the proposed approach is satisfactory. Here the groups of sites are the four regions. The calculation details of these quantities are given in Appendix A-1.

Figure 8 shows the scatter plots of pairwise nonparametric extremal coefficient estimates θ versus the distance (h) for the four regional models. The information in the extremal coefficient reflects the practical number of independent variables (Padoan *et al.*, 2010). $\theta = 1$ indicates complete dependence between two locations, whereas $\theta = 2$ demonstrates full independence.

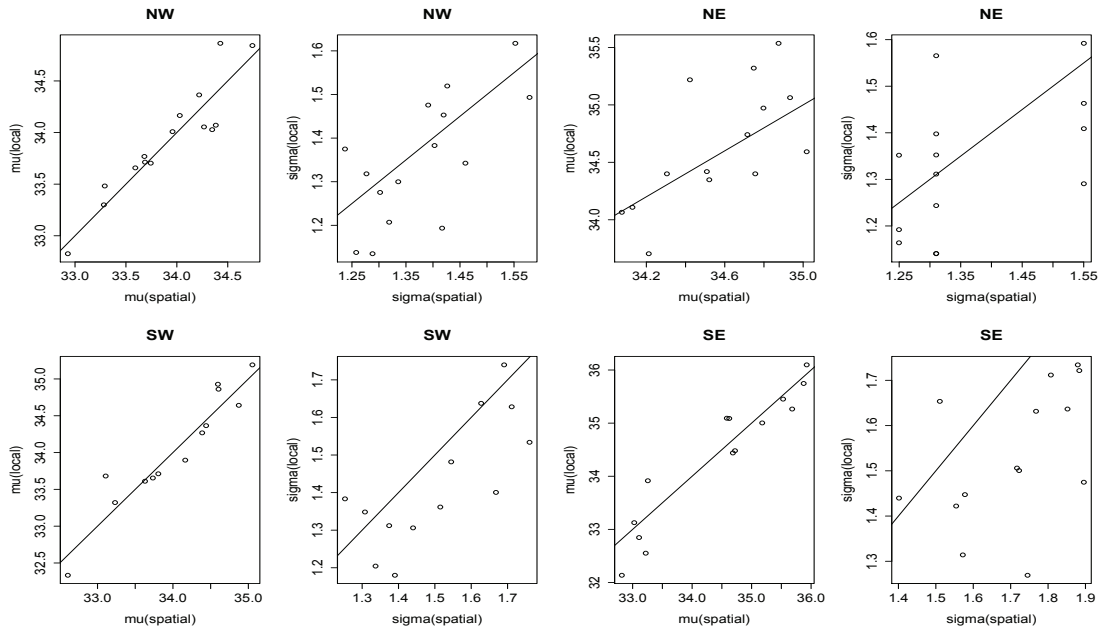


Figure 6: Scatter plots of parameters μ and σ estimated using the MLE method from the independent GEV distribution (vertical axis) and the MSP model (horizontal axis) for four regions (unit: degrees Celsius).

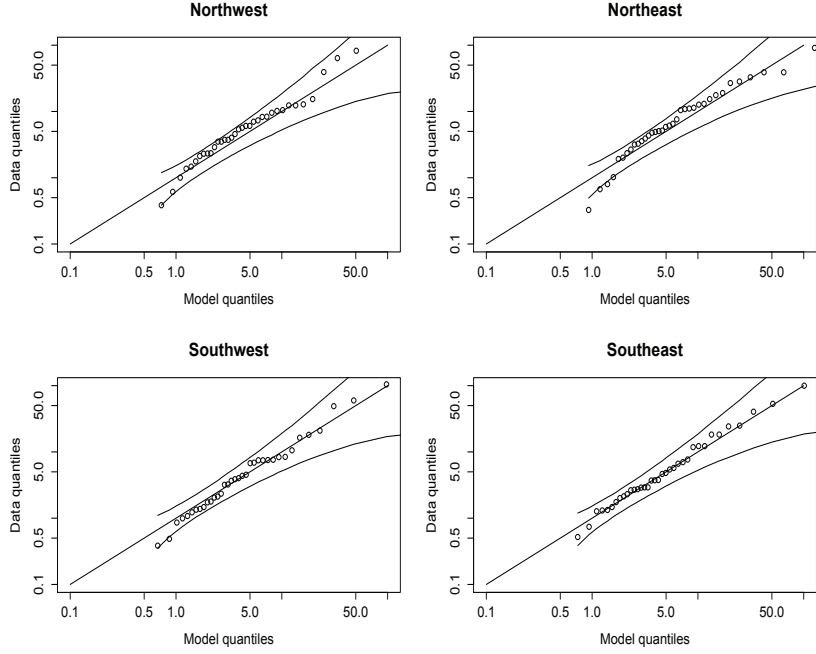


Figure 7: Comparison of groupwise annual maxima with data simulated from fitted models for four regions. The band in each panel indicates the 95% confidence band, and groups of sites indicate four regions.

The lines are the theoretical extremal coefficient function computed by plugging the estimated hyper-parameters into the correlation function. Figure 8 shows moderate spatial dependence and differently increasing tendencies for the four regions, which indicate that regional MSP modeling is more suitable than the independent GEV distribution approach and MSP modeling based on the model for entire region.

4. Results of data analysis

4.1. Estimation of return levels

We calculate the return level of the annual highest temperature for several return periods (5, 10, 25, and 50 years) by using the regional models. Figure 9 shows the results and image maps. The return level for year T , x_T , is the level exceeded only once every T years on average (Coles, 2001).

It is well known that surface air temperature is strongly influenced by local climate factors such as the area's elevation, topography, and soil moisture. However, the annual highest DMT is influenced by local climate factors as well as large-scale weather patterns. An increase in the DMT is typically found on dry soil surfaces with a low albedo. Warming through urbanization can also increase the temperature around the city (Kim and Kim, 2011). As shown in Figure 9, the maximum estimated return levels for the highest DMT are found for basin regions between the Taebaek Mountains in the NE region and the Sobek Mountain in the western region.

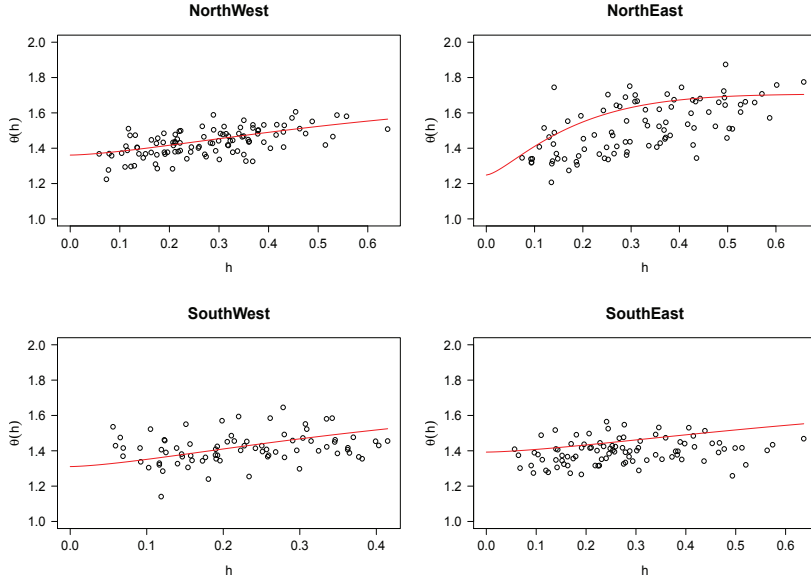


Figure 8: Scatter plots of pairwise nonparametric extremal coefficient estimates θ versus the distance (h) for four regional models. The lines indicate the theoretical extremal coefficient function computed by plugging estimated hyper-parameters into the correlation function.

This is mainly due to the low intensity of rainfall and the low frequency of rainy days as a result of the rain shadow effect of the westerly flow in the middle latitude on these areas. The minimum return values are found for high mountain regions, indicating the effectiveness of the spatial modeling of the highest DMT based on the MSP. *Durre and Wallace (2000)* suggest that synoptic-scale circulation patterns favorable to strong daytime heating and a lack of precipitation may contribute to the relationship between soil moisture and the DMT. They also suggest that as a result of increases in the sensible heat flux from dry soil, record and near-record high temperatures are particularly likely during periods of moisture deficits, implying that land-atmosphere feedback is enhanced during such periods. The rain shadow effect on basin regions may provide favorable conditions for the highest DMT. In Korea, the best conditions for the annual highest DMT are found in August because weather conditions are favorable to high insolation after the rainy season from late June to July.

4.2. Prediction for ungauged location: comparison of three approaches

For the prediction of the return level for an ungauged location (say, x_0), we employ three different methods for comparison purpose; MSP-GEV, MSP-Kriging and GEV-Kriging methods. The first natural one is the MSP-GEV method. Here, we obtain the return level for x_0 by using the formula for univariate GEV distribution, into which we plug the estimates $\hat{\mu}(x_0)$, $\hat{\sigma}(x_0)$, $\hat{\xi}(x_0)$ from the MSP regional model. Figure 9 shows the maps for four return levels. The maps are consisted by 1 km resolution grids. For smooth images around the boundaries of the four regions, we compute the return value for each location around a boundary by using the regional models for the two adjacent regions and then average the values. Ta-

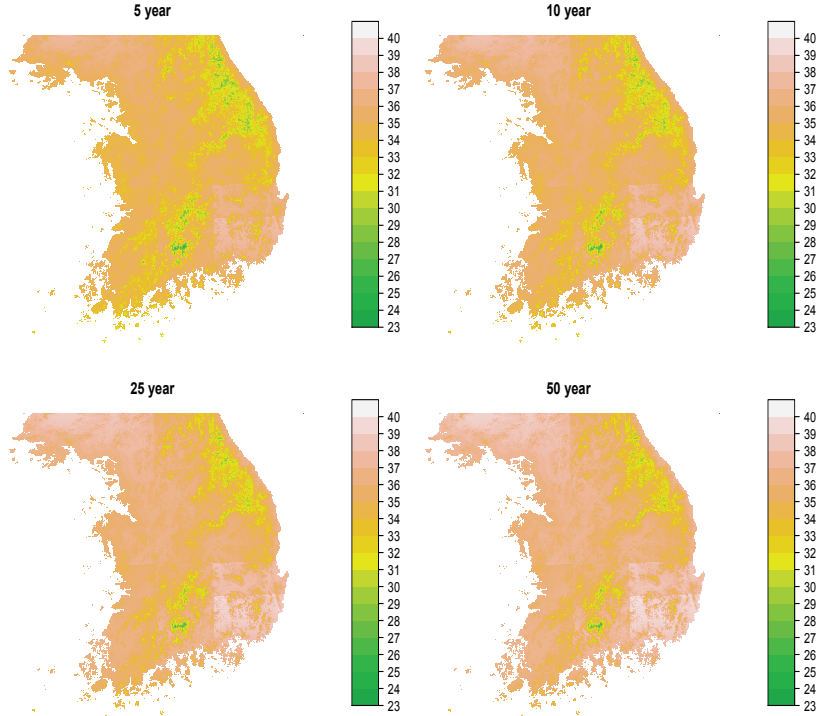


Figure 9: Maps for estimated return levels of the annual highest daily maximum temperature obtained using the MSP-GEV method for several return periods (unit: degrees Celsius). The return values for an ungauged location (e.g., say x_0) are obtained by the formula for univariate GEV distribution with the estimates $\hat{\mu}(x_0)$, $\hat{\sigma}(x_0)$, $\hat{\xi}(x_0)$ of MSP regional models. The resolution of map is obtained by a 1km grids in South Korea.

bles 5 to 8 and Tables 9 to 14 in the Appendix A-2 show the return values and standard errors (in parentheses) for 56 stations and 108 ungauged locations, respectively. As shown in Tables 9 to 14, high-elevation locations (e.g., Taebaek and Jirisan) show relatively low return levels. We obtain the standard errors by using the delta method Coles (2001), which needs a covariance matrix of estimated $\hat{\mu}(x)$, $\hat{\sigma}(x)$, $\hat{\xi}(x)$. It is calculated from the covariance matrix of $\hat{\psi}$; $Cov(\hat{\psi}) = H(\hat{\psi})^{-1} J(\hat{\psi})^{-1} H(\hat{\psi})^{-1}$, which is given in (9).

Figure 10 shows the scatter plots of estimated standard errors of return levels computed from the local (or independent) GEV model (vertical axis) and from the MSP-GEV model (horizontal axis) for various return periods. The estimated standard errors computed from the MSP-GEV model are smaller than those computed from the local GEV model. This may be because the MSP model uses many observations from neighboring stations, whereas the local GEV model uses observations from only one station. This is an advantage of the MSP-GEV model.

The second method we employ is called the MSP-Kriging method, which uses ordinary Kriging to interpolate return levels for ungauged locations by using four geographic variables (latitude, longitude, altitude, and coastal area) and employs return levels for stations obtained from the four regional MSP models. Figure 11 shows the maps. For the correlation function for

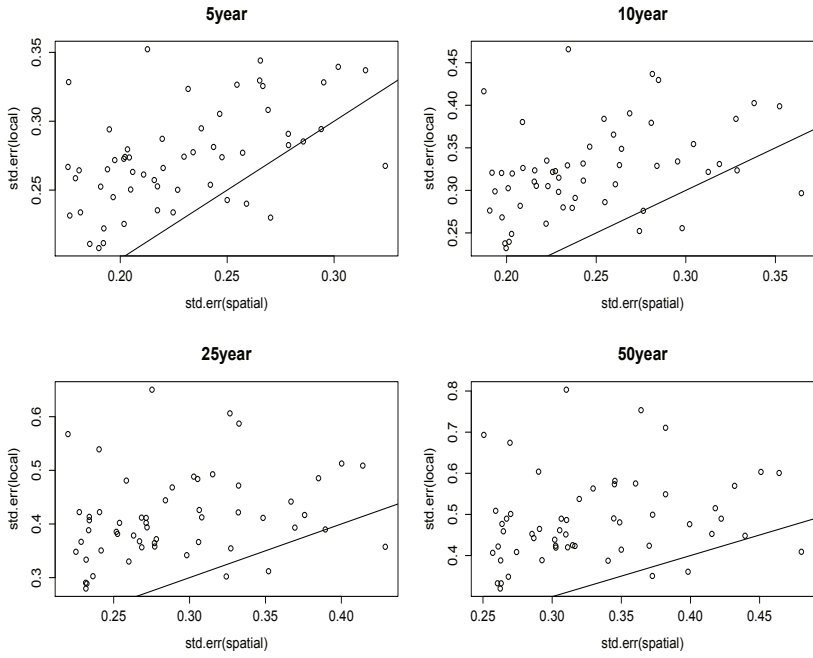


Figure 10: Scatter plots of estimated standard errors of return levels computed from the local GEV model (vertical axis) and the MSP-GEV model (horizontal axis), for various return periods.

Kriging, a power exponential correlation function is used with the four geographical variables;

$$\rho(Y(x_i), Y(x_j)) = \exp\left(-\sum_{k=1}^4 \theta_k |x_{ki} - x_{kj}|^{\alpha_k}\right). \quad (13)$$

We estimate the hyper-parameters (θ_k, α_k) in (13) by using the MLE method in the *DiceKriging* package in R *Roustant et al.* (2012).

The third approach is called the GEV-Kriging method, which computes all return levels for each station from local GEV model and estimates the values of ungauged location through ordinary Kriging. Figure 12 shows the maps. The resolution of map is constructed by 1km grid.

The results in Figures 9, 11 and 12 indicate that the MSP-GEV method can better capture geographical and covariate information than the MSP-Kriging and GEV-Kriging methods. (This decision is based on the experts' eye view, so we do not claim this result be a scientific one and can be applicable to other situations.) Specially, low temperatures around the Taebak and Sobek Mountains are well captured by the MSP-GEV method, whereas they are not captured by the other two methods. However, all three methods well represent temperatures in inland plains and coastal areas. This is because the weather stations are generally located in inland plains and coastal regions, while a few are located in mountain regions. Thus, the MSP modeling of the highest DMT can enhance the reasonableness of spatial patterns of return values and associated indices. Noteworthy is that the MSP-Kriging method does not provide better predictions than the GEV-Kriging method.

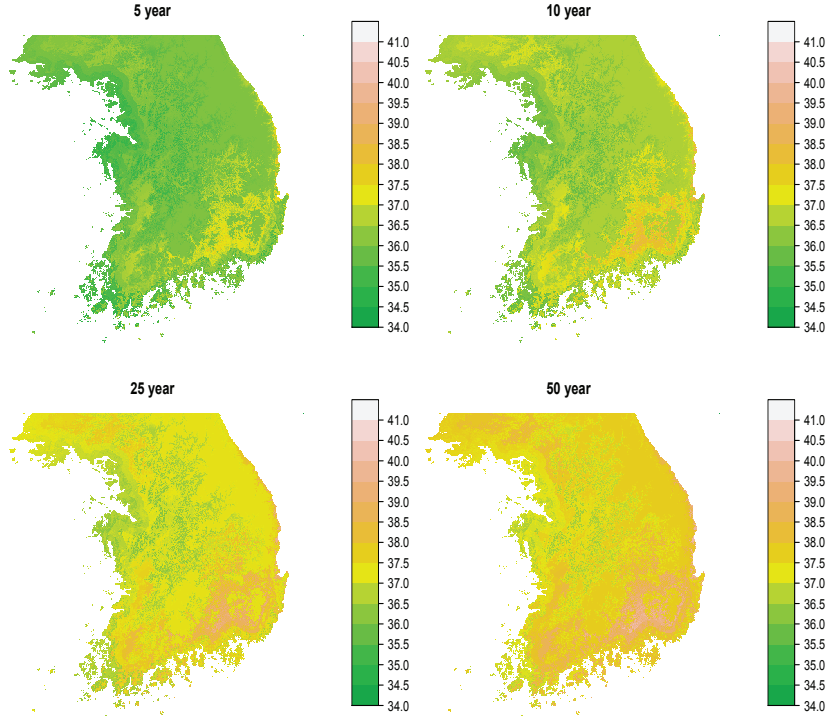


Figure 11: Maps for estimated return levels, obtained by the MSP-Kriging method, of the annual highest daily maximum temperature for several return periods (unit: degrees Celsius). An ordinary Kriging was used to interpolate the return levels at ungauged locations by using 4 geographic variables, where return levels at observation stations are obtained from 4 regional MSP models. The resolution is obtained from every 1km grid locations in South Korea.

4.3. Cluster analysis

We conduct a cluster analysis for the 56 weather stations by using four geographic variables (the latitude, the longitude, the altitude, and the coastal area) and four estimated return levels corresponding to four return periods (5, 10, 25, and 50 years). We employ “complete” hierarchical clustering method, the default method in the *hclust* function in R, to classify the stations into six groups. Figure 13 shows the maps for these six groups, and Table 4 shows the averages of eight variables and geographical configurations for each group. From Table 4, the ascending order of average return levels is as follows:

$$\text{Group 3} \approx \text{Group 4} < \text{Group 6} < \text{Group 2} < \text{Group 1} < \text{Group 5}.$$

The maximum averages of return levels are found for plains in the southeastern region (Group 5). Noteworthy is that the average return levels for west coastal region (Group 3) and inland mountain region (Group 4) are almost the same as the minimum averages for the six groups.

Figure 13 shows three groups, respectively, in inland and coastal areas. In particular, Group 4 (located in inland areas) is related mainly to the altitude. In fact, as shown in Table 4, Group 4 shows the highest altitude value (215.7 meter) and the lowest return level for each return period.

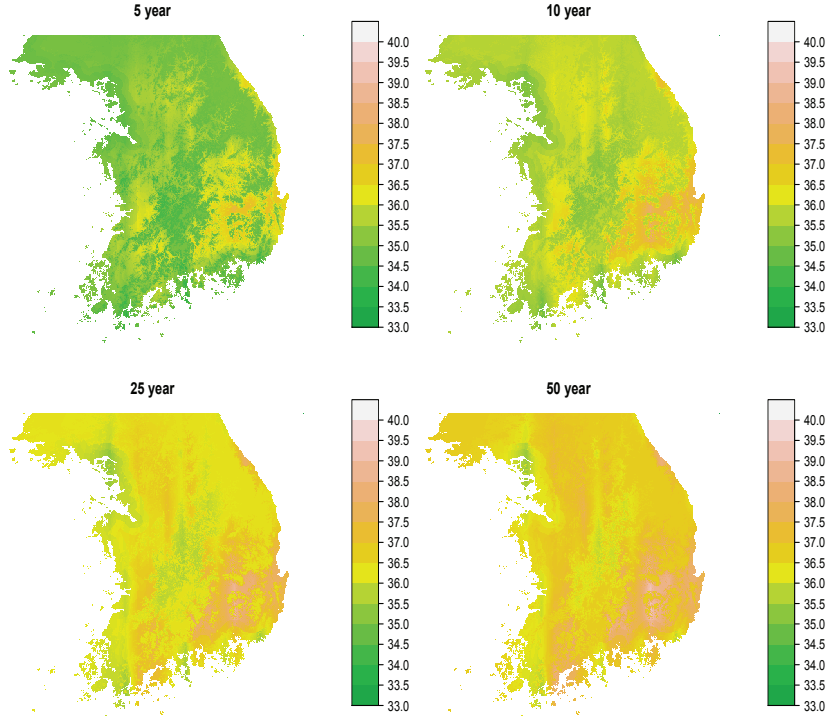


Figure 12: Maps for the estimated return levels, of the annual highest of daily maximum temperature obtained using the GEV-Kriging method, for several return periods. We employ ordinary Kriging to interpolate return levels for ungauged locations by using four geographic variables. Return levels at observation stations are obtained from local GEV models and 1km resolution grid.

The most interesting group is Group 5, which shows the highest return level. This may be due to low altitudes, low latitudes, and inland basin regions, which provide favorable conditions for surface heating when there are synoptic situations. Previous studies have shown that this region is characterized by the low frequency of rainy days (*Ko et al.*, 2005; *Kim et al.*, 2005).

Table 4: The averages of eight variables (latitude, longitude, altitude, distance to coast, 5-year return level, 10-year return level, 25-year return level, and 50-year return level) based on the cluster analysis, and the geographic configuration for each group ('rl' indicates the return level).

group	latit.	longit.	altit.	coast	5yr-rl	10yr-rl	25yr-rl	50yr-rl	Geograph. config.
1	37.38	129.0	34.85	1.00	36.60	37.28	37.96	38.36	northeast coast
2	36.37	127.65	91.77	4.79	36.29	36.93	37.58	37.96	inland plain
3	36.14	126.60	32.01	1.44	35.19	35.91	36.64	37.09	west coast
4	36.60	127.80	215.7	5.66	35.44	36.03	36.63	36.99	inland mountain
5	35.65	128.67	31.92	3.80	37.57	38.27	38.96	39.36	southeast plain
6	35.03	128.02	40.46	1.00	35.61	36.39	37.16	37.62	southern coast

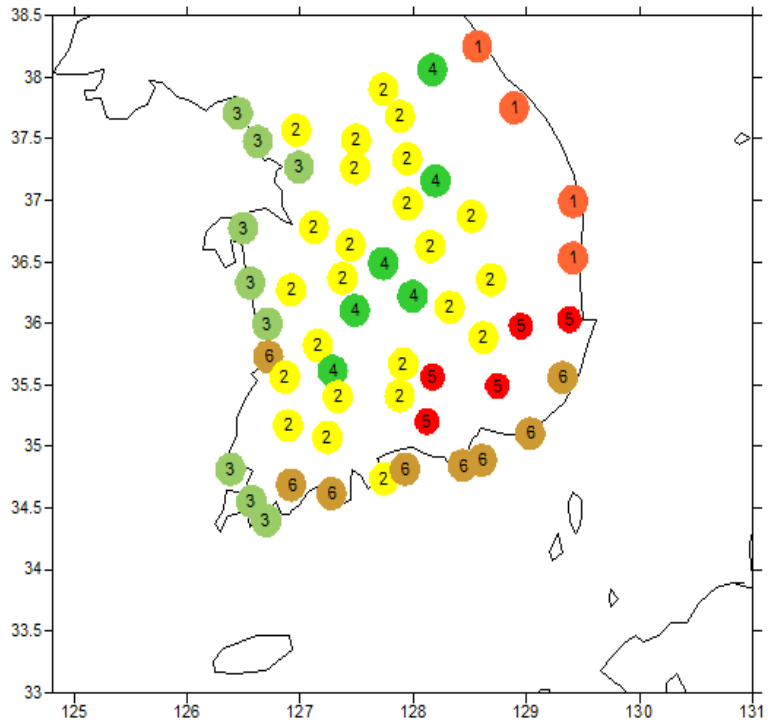


Figure 13: Map for six groups obtained through a cluster analysis using four geographic variables and four return levels for 56 stations.

5. Summary and discussion

In this study, we apply a spatial modeling technique, max-stable processes (MSP) model, to the highest annual temperature in Korea. We use Schlather's characterization with a powered exponential correlation function. We build four regional models. Figure 4 and Figure 5 show the q-q plots for the same stations, which indicate that the four regional models provide a better fit to the data for most stations than the model for entire region. In addition, we compute the return levels of the highest annual temperature for several return periods by using the regional models and draw maps based on the return levels. A comparison of the maps of predicted return levels computed through three different methods indicates the superiority of MSP modeling over the GEV model and Kriging. In addition, we conduct a cluster analysis for 56 weather stations by using geographic variables and estimated return levels and present a geographical configuration.

We set the shape parameter to be a constant, and thus, future research could consider a non-constant shape parameter $\xi(x)$, which may require more sample. We enhance the MSP model by partitioning the country into four regions, but the partitioning is somewhat arbitrary. That is, we partition the country based on our expertise, administrative information, and geographical proximity. Thus, there is a need for assigning weather stations to various regions in a systematic manner. *Coles* (1993) discusses this issue and recommends the use of nonparametric estimates of extremal coefficients (*Smith*, 1990). In this regard, some techniques for analyzing regional frequency may be useful (e.g., *Hosking and Wallis* (1997)).

Building the best regression-based form for location and scale parameters requires substantial computational burdens. We select the covariates at the minimum TIC from many possible regression-based forms. Actually, we employ a stagewise selection procedure to select the best regression-based form from all possible combinations. However, we observe the failure of the TIC computation in a few cases, which makes the procedure unstable. *Westra and Sisson* (2011) took a forward selection approach by employing a likelihood ratio test. *Varin and Vidoni* (2005) discussed on selecting a model that minimizes the composite likelihood information criterion (CLIC). In this regard, future research should develop a fast and stable algorithm for the better selection of variables.

To compute the standard errors of return levels, we employ the delta method. Because the delta method requires a large sample, the estimates of standard errors are likely to be underestimated for a small sample. Thus, as an alternative and for obtaining confidence intervals, the bootstrap method can be used parametrically. A nonparametric bootstrap method may not be directly applicable because replicated spatial observations obtained by sampling with replacement make the covariance matrix singular. In addition, the profile likelihood method may not be directly applicable. We leave this issue to future research.

This study's proposed approach can be applied to field of numerical model output of climate systems and compared with a model fitted to climate observations. In this regard, future research will serve the detection and prediction of changes in the climate, including trends in extreme temperatures (*Lee et al.*, 2011). In addition, an MSP model allowing for temporality should be useful. Idea of *Stephenson and Tawn* (2005), used again by *Davison* (2009), may be useful for modeling spatiotemporal extreme events and detecting changes in such events. Drawbacks and possible future developments of the MSP modeling approach were discussed in *Davison and Gholamrezaee* (2012).

Modeling the entire distribution (including maxima, mean and minima simultaneously) of a climate variable for a spatial field and using it to detect changes (e.g., shifts in means and standard deviations) may be more reliable and valuable than modeling only extremes (*Katz*, 2010). For this purpose, a time-dependent MSP model as well as a spatiotemporal linear model based on the Gaussian processes (*Cressie and Wikle*, 2011) can be useful. Addressing these challenges requires increased collaboration between climate scientists and statisticians.

Acknowledgments

The authors are grateful to M. Mehdi Gholamrezaee for his technical report and help in R programming. This paper is motivated by the last author's participation in the Workshop on Spatial Extremes and Applications at EPFL, Lausanne, Switzerland, in July 2009. He would like to thank Professor Anthony Davison and the workshop staff for their hospitality and support. The authors are very much indebted to reviewers who have provided constructive and valuable comments to improve this paper. This work was supported by the National Institute of Meteorological Research, Korea.

References

- Beirlant, J., Y. Goegebeur, J. Segers, and J. Teugels (2004), *Statistics of Extremes: Theory and Applications*, Wiley, N.Y.
- Blanchet, J., and A. Davison (2011), Spatial modeling of extreme snow depth, *Annals of Applied Statistics*, 5, 1699–1725.
- Buishand, T.A., L. de Haan, and C. Zhou (2008), On spatial extreme: With application to a rainfall problem, *Annals of Applied Statistics*, 2(2), 624–642.
- Caesar, J., L. Alexander, and R. Vose (2006), Large-scale changes in observed daily maximum and minimum temperatures: Creation and analysis of a new gridded data set, *J. Geophys. Res.*, 111, D05101, doi:10.1029/2005JD006280.
- Choi, G., Collins, D., Ren, G., Trewin, B., Baldi, M., Fukuda, Y., Afzaal, M., Pianmana T., et al. (2009), Changes in means and extreme events of temperature and precipitation in the Asia-Pacific network region, 1955–2007, *Int. J. Climatol.*, 29, 1906–1925.
- Coles, S. (1993), Regional modelling of extreme storms via max-stable processes, *J. Roy. Statist. Soc. B*, 55, 797–816.
- Coles, S. (2001), *An Introduction to Statistical Modelling of Extreme Values*, Springer, N.Y.
- Coles, S.G., and J.A. Tawn (1991), Modeling extreme multivariate events, *J. Roy. Statist. Soc. B*, 53, 377–392.
- Coles, S.G., and D. Walshaw (1994), Directional modelling of extreme wind speeds, *J. Roy. Statist. Soc. C: Appl. Statist.*, 43, 139–157.
- Cressie, N., and C. Wikle (2011), *Statistics for spatio-temporal data*, Wiley, Hoboken.
- Davison, A.C. (2009), A Sketch of Statistics of Spatial Extremes, A lecture note given at the Workshop on Spatial Extremes and Applications, EPFL, Lausanne, Switzerland, <http://extremes.epfl.ch/files/content/sites/extremes/files/users/111184/public/> WorkshopJuly09/Davison.pdf [accessed 5 Mar. 2012].
- Davison, A.C., and M.M. Gholamrezaee (2012), Geostatistics of extremes, *Proceedings of the Royal Society A*, doi:10.1098/rspa.2011.0412
- DeGaetano, A., and R. Allen (2002), Trends in twentieth century extremes across the United States, *Jour. Climate*, 15, 3188–3205.
- de Haan, L. (1984), A spectral representation for max-stable processes, *Annals of Probability*, 12(4), 1194–1204.
- de Haan, L. (1985), Extremes in higher dimensions: the model and some statistics, In: proceedings of the 45th Session of the International Statistical Institute, Paper 26.3. International Statistical Institute, The Hague.
- de Haan, L., and T. Lin(2003), Weak consistency of extreme value estimators in $C[0,1]$, *Ann. Statist*, 31, 1996–2012.
- de Haan, L., and T.T. Pereira (2006), Spatial extremes: models for the stationary case, *Ann. Statist*, 34, 146–168.
- de Haan L., and S.I. Resnick, (1977), Limit theory for multivariate sample extremes, *Z. Wahrs. verw. Gebiete*, 40, 317–337.
- Durre, I., and J.M. Wallace (2000), Dependence of Extreme Daily Maximum Temperatures on Antecedent Soil Moisture in the Contiguous United States during Summer, *Journal of Climate*, 13, 2641–2651.
- Easterling, D.R., H. Briony, D.J. Philip, C.P. Thomas, R.K. Thomas, E.P. David, M.J. Salinger, V. Razuvayev, N. Plummer, P. Jamason, and C.K. Folland (1997), Maximum and minimum temperature trends for the globe, *Science*, 277, 364–367.

- Gholamrezaee, M.M. (2009), Diagnostic tools in spatial modeling of extreme values, Workshop on Spatial Extremes and Applications, EPFL, Lausanne: Switzerland, <http://extremes.epfl.ch/webdav/site/extremes/users/> [accessed 30 Sept. 2010].
- Hongmei, L., T. Zhou, and J. Nam, 2009: Comparison of daily extreme temperatures over Eastern China and South Korea between 1996-2005, *Advances in Atmos. Sci.*, **26**(2), 253-264.
- Hopkinson, R.F., D.W. McKenney, E.J. Milewska, M.F. Hutchinson, P. Papadopol, and L.A. Vincent (2011), Impact of aligning climatological day on gridding daily maximum-minimum temperature and precipitation over Canada, *J. Appl. Meteor. Climatol.*, **50**, 1654–1665.
- Hosking, J.R.M., and J.R. Wallis (1997), *Regional frequency analysis: An approach based on L-moments*, Cambridge University Press, Cambridge.
- Hüsler J. (2009), Extreme value analysis in biometrics, *Biometrical Journal*, **51**, 252–272.
- Kabluchko, Z., M. Schlather, and L. de Haan (2009), Stationary max-stable fields associated to negative definite functions, *Annals of Probability*, **37**, 2042–2065.
- Karl, T.R., P.D. Jones, R.W. Knight, G. Kukla, N. Plummer, V. Razuvayev, K.P. Gallo, J. Lindseay, R.J. Charlson, and T.C. Peterson (1993), A new perspective on recent global warming: asymmetric trends of daily maximum and minimum temperature, *Bull. Amer. Meteor. Soc.*, **74**, 1007–1023.
- Katz, R.W. (2010), Statistics of extremes in climate change, *Climatic Change*, **100**, 71–76.
- Korea Meteorological Administration (KMA) (2010), Abnormal Climate Extreme Special Report 2010. 114p.
- Kim E.-H., M.-K. Kim, and W.-S. Lee (2005), The regional characteristics of daily Precipitation intensity in Korea for recent 30 Years, *Jour. Korea Earth Sci. Soc.*, **26**, 404–416.
- Kim M.-K. and S. Kim (2011), Quantitative Estimates of Warming by Urbanization in South Korea ove the Past 55 Years (1955-2008), *Atmospheric Environment*, **45**, 5778–5783. doi:10.1016/j.atmosenv.2011.07.028.
- Ko, J.-W., H.-J. Baek, and W.-T. Kwon (2005), The characteristics of precipitation and regionalization during rainy season in Korea, *J. Kor. Meteorol. Soc.*, **41**, 101–114.
- Kotz, S., and S. Nadarajah (1999), *Extreme Value Distributions: Theory and Applications*, Imperial College Press, London.
- Lee, T.C., H.S. Chan, E.W.L. Ginn, and M.C. Wong, 2011: Lomng-term trends in extreme temperatures in Hong Kong and Southern China, *Advances in Atmos. Sci.*, **28**(1), 147-157.
- Padoan, S.A., M. Ribatet, and S.A. Sisson (2010), Likelihood-based inference for max-stable processes, *Journal of the American Statistical Association*, **105**, 263–277.
- Parey, S., F. Malek, C. Laurent, and D. Dacunha-Castelle (2007), Trends and climate evolution: Statistical approach for very high temperatures in France, *Climatic Change*, **81**, 331–352.
- Resnick, S. (2007), *Heavy-tail Phenomena*, Springer, N.Y.
- Ribatet, M. (2009), A User's Guide to the SpatialExtremes Package, <http://spatialextremes.r-forge.r-project.org/docs/SpatialExtremesGuide.pdf> [accessed 30 Sept 2010].
- Robinson, D.A., D.J. Leathers, M.A. Palecki, and K.F. Dewey (1995), Some observations on climate variability as seen in daily temperature structure, *Atmos. Res.*, **37**, 119–131.
- Roustant, O., D. Ginsbourger, and Y. Deville (2012), DiceKriging, DiceOptim: Two R packages for the analysis of computer experiments by kriging-based metamodeling and optimization, *Jour. Statistical Software*, To appear.
- Sang, H.Y., and A.E. Gelfand (2010), Continuous Spatial Process Models for Spatial Extreme Values, *Journal of Agricultural, Biological, and Environmental Statistics*, **15**, 49–65.
- Schlather, M. (2002), Models for stationary max-stable random fields, *Extremes*, **5**, 33–44.

- Schlather, M., and J.A. Tawn (2003), A dependence measure for multivariate and spatial extreme values: Properties and inference, *Biometrika*, 90, 139–156.
- Smith, R.L. (1990), Max-stable processes and spatial extremes, unpublished manuscript, <http://www.stat.unc.edu/postscript/rs/spatex.pdf> [accessed 5 Oct 2010].
- Stephenson, A. and J. Tawn (2005), Exploiting occurrence times in likelihood inference for component-wise maxima, *Biometrika*, 92, 213–227.
- USCCP (2008), *Weather and climate extremes in a changing climate*. 162pp.
- Varin, C. and P. Vidoni (2005), A note on composite likelihood inference and model selection, *Biometrika*, 92, 519–528.
- Westra, S., and S.A. Sisson (2011), Detection of non-stationarity in precipitation extremes using a max-stable process model, *Journal of Hydrology*, 406, 119–128.
- Zhang, Z., and R.L. Smith (2010), On the estimation and application of max-stable processes, *Jour. Statist. Plan. Infer.*, 140, 1135–1153.

Appendix A-1: Computation of a quantile-per-quantile plot of groupwise maxima from data and model

To compute the quantiles for the model and data, we employ the following procedure for each region. To obtain groupwise maxima and data quantiles, we first transform the observations for weather station x by using the Frèchet transformation (7) with $\hat{\mu}(x)$, $\hat{\sigma}(x)$, $\hat{\xi}(x)$. We do this for all 56 stations and select the maximum from 56 values. We repeat this procedure for 37 years of data. We then obtain the data quantiles by sorting 37 maxima in ascending order.

For computing model quantiles, we first generate a max-stable random field having a powered exponential correlation function (6) with the estimated parameters $(\hat{\nu}, \hat{\tau}, \hat{\eta})$ for 37 years by using the *rmaxstab* function in *SpatialExtremes* in R Ribatet (2009). We then obtain 37 groupwise maxima and sort them in ascending order. We repeat this B times (e.g., 1,000 times) to have B sets of 37 maxima. By averaging the ordered maxima over B sets for each year, we obtain 37 average maxima providing model quantiles. We obtain the $100(1 - \alpha)\%$ confidence interval for each year by selecting $(\frac{\alpha}{2} \times B)$ -th and $(100(1 - \frac{\alpha}{2}) \times B)$ -th observations from B simulated maxima for the year.

Appendix A-2: Tables of parameter estimates and return levels for 56 observation stations and 108 unobserved locations

Table 5: Geographic information (latitude, longitude, altitude, distance to coast, and geographic region) for 56 observed locations and estimated parameters with standard errors in parenthesis from the 4 regional models via max-stable processes (unit: degree Celsius).

Location	Latit.	longit.	altit.	coast	region	location		scale		shape	
Sokcho	38.25	128.56	22	2	NE	34.78	(0.19)	1.49	(0.11)	-0.30	(0.05)
Chuncheon	37.90	127.74	76	3	NE	35.11	(0.24)	1.44	(0.11)	-0.30	(0.05)
Gangneung	37.75	128.89	25	4	NE	35.41	(0.21)	1.39	(0.10)	-0.30	(0.05)
Seoul	37.57	126.97	85	3	NW	33.30	(0.22)	1.43	(0.12)	-0.24	(0.05)
Incheon	37.48	126.62	69	7	NW	34.76	(0.21)	1.29	(0.11)	-0.24	(0.05)
Wonju	37.34	127.95	150	2	NE	34.65	(0.29)	1.49	(0.11)	-0.30	(0.05)
Suwon	37.27	126.99	34	5	NW	34.29	(0.21)	1.36	(0.11)	-0.24	(0.05)
Chungju	36.97	127.95	113	7	NE	34.45	(0.25)	1.24	(0.10)	-0.30	(0.05)
Seosan	36.77	126.50	25	7	NW	35.64	(0.21)	1.18	(0.11)	-0.24	(0.05)
Uljin	36.99	129.41	49	3	NE	34.55	(0.21)	1.44	(0.11)	-0.30	(0.05)
Cheongju	36.64	127.44	56	6	NW	35.11	(0.21)	1.22	(0.11)	-0.24	(0.05)
Daejeon	36.37	127.37	62	4	NW	34.39	(0.21)	1.29	(0.11)	-0.24	(0.05)
Chupungyeong	36.22	127.99	240	5	NW	33.65	(0.21)	1.25	(0.11)	-0.24	(0.05)
Pohang	36.03	129.38	1	3	SE	36.17	(0.24)	1.47	(0.13)	-0.28	(0.05)
Gunsan	36.00	126.71	25	1	SW	32.96	(0.26)	1.57	(0.12)	-0.27	(0.06)
Daegu	35.89	128.62	57	6	SE	33.79	(0.28)	1.96	(0.22)	-0.28	(0.05)
Jeonju	35.82	127.16	61	8	SW	34.44	(0.26)	1.57	(0.12)	-0.27	(0.06)
Ulsan	35.56	129.32	34	4	SE	33.17	(0.27)	1.90	(0.20)	-0.28	(0.05)
Gwangju	35.17	126.89	70	5	SW	32.61	(0.27)	1.57	(0.12)	-0.27	(0.06)
Busan	35.10	129.03	69	4	SE	32.91	(0.26)	1.87	(0.20)	-0.28	(0.05)
Tongyeong	34.85	128.44	30	5	SE	29.21	(0.47)	2.36	(0.31)	-0.28	(0.05)
Mokpo	34.82	126.38	37	8	SW	29.79	(0.36)	1.89	(0.16)	-0.27	(0.06)
Yeosu	34.74	127.74	73	5	SE	29.30	(0.48)	2.32	(0.31)	-0.28	(0.05)
Wando	34.40	126.70	27	2	SW	29.87	(0.36)	1.89	(0.16)	-0.27	(0.06)
Jinju	35.21	128.12	21	3	SE	34.06	(0.28)	1.87	(0.19)	-0.28	(0.05)
Ganghwa	37.71	126.45	46	4	NW	33.88	(0.21)	1.39	(0.11)	-0.24	(0.05)

Table 6: Table 5 continued

Location	Latit.	longit.	altit.	coast	region	location	scale	shape
Yangpyeong	37.49	127.49	47	6	NW	34.55 (0.21)	1.32 (0.11)	-0.24 (0.05)
Icheon	37.26	127.48	90	7	NW	34.63 (0.21)	1.29 (0.11)	-0.24 (0.05)
Inje	38.06	128.17	198	3	NE	33.82 (0.21)	1.44 (0.11)	-0.30 (0.05)
Hongcheon	37.68	127.88	146	6	NE	34.84 (0.21)	1.29 (0.10)	-0.30 (0.05)
Jecheon	37.16	128.19	263	5	NE	34.10 (0.21)	1.34 (0.10)	-0.30 (0.05)
Boeun	36.49	127.73	173	7	NW	34.74 (0.21)	1.18 (0.11)	-0.24 (0.05)
Cheonan	36.78	127.12	21	5	NW	34.98 (0.21)	1.25 (0.11)	-0.24 (0.05)
Boryeong	36.33	126.56	17	7	NW	35.69 (0.21)	1.18 (0.11)	-0.24 (0.05)
Buyeo	36.27	126.92	11	5	NW	35.04 (0.21)	1.25 (0.11)	-0.24 (0.05)
Geumsan	36.11	127.48	170	2	NW	33.05 (0.23)	1.36 (0.11)	-0.24 (0.05)
Buan	35.73	126.72	3	2	SW	33.13 (0.26)	1.57 (0.12)	-0.27 (0.06)
Imsil	35.61	127.29	248	3	SW	33.00 (0.27)	1.57 (0.12)	-0.27 (0.06)
Jeongeup	35.56	126.87	39	6	SW	32.85 (0.27)	1.57 (0.12)	-0.27 (0.06)
Namwon	35.41	127.33	93	6	SW	34.20 (0.26)	1.57 (0.12)	-0.27 (0.06)
Suncheon	35.08	127.24	74	2	SW	34.34 (0.26)	1.57 (0.12)	-0.27 (0.06)
Jangheung	34.69	126.92	44	6	SW	29.74 (0.36)	1.89 (0.16)	-0.27 (0.06)
Haenam	34.55	126.57	4	4	SW	30.05 (0.36)	1.89 (0.16)	-0.27 (0.06)
Goheung	34.62	127.28	53	5	SW	31.44 (0.36)	1.89 (0.16)	-0.27 (0.06)
Yeongju	36.87	128.52	210	4	NE	33.74 (0.31)	1.39 (0.10)	-0.30 (0.05)
Mungyeong	36.63	128.15	170	2	NE	33.88 (0.36)	1.49 (0.11)	-0.30 (0.05)
Yeongdeok	36.53	129.41	41	8	NE	34.80 (0.30)	1.19 (0.10)	-0.30 (0.05)
Uiseong	36.36	128.69	82	5	NE	34.51 (0.23)	1.34 (0.10)	-0.30 (0.05)
Gumi	36.13	128.32	47	3	NE	34.62 (0.26)	1.44 (0.11)	-0.30 (0.05)
Yeongcheon	35.98	128.95	93	4	SE	33.52 (0.27)	1.86 (0.19)	-0.28 (0.05)
Geochang	35.67	127.91	221	2	SE	32.97 (0.28)	1.69 (0.18)	-0.28 (0.05)
Hapcheon	35.57	128.17	33	7	SE	33.97 (0.28)	2.01 (0.24)	-0.28 (0.05)
Miryang	35.49	128.74	10	6	SE	34.14 (0.29)	1.99 (0.23)	-0.28 (0.05)
Sancheong	35.41	127.88	138	7	SE	33.60 (0.28)	1.94 (0.23)	-0.28 (0.05)
Geoje	34.89	128.60	44	2	SE	29.10 (0.48)	2.23 (0.27)	-0.28 (0.05)
Namhe	34.82	127.93	43	2	SE	29.53 (0.47)	2.23 (0.27)	-0.28 (0.05)

Table 7: Return levels for several return periods (standard errors in parenthesis) for 56 observed locations (unit: degree Celsius).

Location	5 year	10 year	25 year	50 year	100 year	200 year
Sokcho	36.58 (0.25)	37.22 (0.29)	37.85 (0.33)	38.21 (0.35)	38.51 (0.37)	38.74 (0.38)
Chuncheon	36.85 (0.31)	37.47 (0.34)	38.08 (0.37)	38.43 (0.40)	38.71 (0.41)	38.94 (0.43)
Gangneung	37.09 (0.26)	37.69 (0.29)	38.28 (0.32)	38.61 (0.34)	38.89 (0.35)	39.11 (0.37)
Seoul	35.10 (0.30)	35.78 (0.36)	36.49 (0.44)	36.91 (0.51)	37.27 (0.58)	37.57 (0.64)
Incheon	36.38 (0.28)	36.99 (0.33)	37.63 (0.41)	38.01 (0.47)	38.33 (0.53)	38.60 (0.58)
Wonju	36.45 (0.36)	37.09 (0.40)	37.72 (0.43)	38.08 (0.45)	38.37 (0.47)	38.61 (0.49)
Suwon	36.00 (0.29)	36.65 (0.34)	37.32 (0.42)	37.72 (0.49)	38.06 (0.55)	38.35 (0.61)
Chungju	35.95 (0.28)	36.48 (0.30)	37.01 (0.33)	37.31 (0.35)	37.55 (0.36)	37.75 (0.37)
Seosan	37.12 (0.27)	37.68 (0.32)	38.27 (0.39)	38.62 (0.45)	38.91 (0.50)	39.16 (0.56)
Uljin	36.29 (0.26)	36.91 (0.29)	37.52 (0.32)	37.87 (0.34)	38.15 (0.36)	38.38 (0.38)
Cheongju	36.64 (0.28)	37.22 (0.33)	37.82 (0.40)	38.18 (0.45)	38.49 (0.51)	38.74 (0.56)
Daejeon	36.01 (0.29)	36.63 (0.34)	37.26 (0.41)	37.64 (0.47)	37.97 (0.53)	38.24 (0.59)
Chupungyeong	35.23 (0.28)	35.83 (0.33)	36.44 (0.40)	36.82 (0.46)	37.13 (0.52)	37.40 (0.57)
Pohang	37.97 (0.29)	38.62 (0.32)	39.27 (0.33)	39.65 (0.33)	39.97 (0.32)	40.22 (0.29)
Gunsan	34.90 (0.33)	35.62 (0.36)	36.34 (0.39)	36.77 (0.39)	37.12 (0.39)	37.41 (0.38)
Daegu	36.19 (0.38)	37.06 (0.45)	37.92 (0.50)	38.43 (0.52)	38.85 (0.53)	39.19 (0.52)
Jeonju	36.39 (0.33)	37.10 (0.37)	37.83 (0.39)	38.25 (0.40)	38.61 (0.40)	38.90 (0.39)
Ulsan	35.50 (0.38)	36.34 (0.43)	37.18 (0.48)	37.67 (0.49)	38.08 (0.49)	38.41 (0.48)
Gwangju	34.55 (0.33)	35.27 (0.36)	35.99 (0.39)	36.42 (0.39)	36.77 (0.39)	37.06 (0.38)
Busan	35.20 (0.38)	36.03 (0.43)	36.86 (0.47)	37.35 (0.49)	37.75 (0.48)	38.07 (0.47)
Tongyeong	32.09 (0.62)	33.14 (0.71)	34.18 (0.79)	34.79 (0.82)	35.29 (0.84)	35.70 (0.85)
Mokpo	32.13 (0.44)	32.99 (0.48)	33.85 (0.51)	34.37 (0.53)	34.79 (0.53)	35.14 (0.52)
Yeosu	32.15 (0.59)	33.18 (0.67)	34.21 (0.75)	34.81 (0.78)	35.30 (0.80)	35.71 (0.81)
Wando	32.20 (0.44)	33.06 (0.48)	33.93 (0.51)	34.44 (0.53)	34.87 (0.53)	35.21 (0.52)
Jinju	36.35 (0.36)	37.18 (0.40)	38.01 (0.44)	38.50 (0.45)	38.89 (0.44)	39.22 (0.42)
Ganghwa	35.63 (0.30)	36.30 (0.35)	36.98 (0.43)	37.40 (0.50)	37.75 (0.56)	38.04 (0.63)

Table 8: Table 7 continued

Location	5 year	10 year	25 year	50 year	100 year	200 year
Yangpyeong	36.22 (0.28)	36.85 (0.34)	37.50 (0.41)	37.89 (0.48)	38.22 (0.54)	38.50 (0.60)
Icheon	36.25 (0.28)	36.87 (0.33)	37.50 (0.41)	37.88 (0.46)	38.21 (0.53)	38.48 (0.58)
Inje	35.56 (0.28)	36.18 (0.31)	36.79 (0.35)	37.14 (0.37)	37.42 (0.39)	37.65 (0.40)
Hongcheon	36.40 (0.26)	36.96 (0.28)	37.50 (0.32)	37.82 (0.33)	38.07 (0.35)	38.27 (0.36)
Jecheon	35.72 (0.27)	36.30 (0.31)	36.86 (0.34)	37.19 (0.36)	37.45 (0.38)	37.66 (0.39)
Boeun	36.23 (0.27)	36.79 (0.32)	37.37 (0.39)	37.72 (0.44)	38.02 (0.50)	38.27 (0.55)
Cheonan	36.55 (0.28)	37.15 (0.33)	37.77 (0.41)	38.14 (0.46)	38.46 (0.52)	38.72 (0.58)
Boryeong	37.17 (0.28)	37.73 (0.32)	38.31 (0.39)	38.67 (0.45)	38.96 (0.50)	39.21 (0.56)
Buyeo	36.61 (0.28)	37.21 (0.33)	37.83 (0.41)	38.20 (0.46)	38.52 (0.52)	38.78 (0.58)
Geumsan	34.77 (0.30)	35.42 (0.36)	36.09 (0.43)	36.49 (0.49)	36.83 (0.56)	37.12 (0.62)
Buan	35.07 (0.33)	35.79 (0.36)	36.51 (0.39)	36.94 (0.39)	37.29 (0.39)	37.58 (0.38)
Imsil	34.94 (0.34)	35.66 (0.37)	36.38 (0.39)	36.81 (0.40)	37.16 (0.40)	37.45 (0.39)
Jeongeup	34.79 (0.33)	35.51 (0.36)	36.23 (0.39)	36.66 (0.39)	37.01 (0.39)	37.30 (0.38)
Namwon	36.14 (0.33)	36.86 (0.36)	37.58 (0.39)	38.01 (0.40)	38.36 (0.39)	38.65 (0.39)
Suncheon	36.29 (0.33)	37.00 (0.36)	37.73 (0.39)	38.15 (0.40)	38.51 (0.40)	38.80 (0.39)
Jangheung	32.07 (0.44)	32.93 (0.48)	33.80 (0.51)	34.31 (0.53)	34.73 (0.53)	35.08 (0.52)
Haenam	32.38 (0.44)	33.24 (0.48)	34.11 (0.51)	34.62 (0.52)	35.04 (0.53)	35.39 (0.52)
Goheung	33.77 (0.45)	34.63 (0.49)	35.49 (0.52)	36.01 (0.53)	36.43 (0.54)	36.78 (0.53)
Yeongju	35.42 (0.37)	36.02 (0.40)	36.60 (0.43)	36.94 (0.45)	37.21 (0.47)	37.43 (0.48)
Mungyeong	35.68 (0.43)	36.32 (0.46)	36.95 (0.49)	37.31 (0.51)	37.60 (0.53)	37.84 (0.54)
Yeongdeok	36.25 (0.27)	36.76 (0.27)	37.26 (0.28)	37.55 (0.29)	37.79 (0.29)	37.98 (0.30)
Uiseong	36.13 (0.28)	36.71 (0.31)	37.27 (0.34)	37.60 (0.35)	37.86 (0.37)	38.07 (0.38)
Gumi	36.36 (0.32)	36.98 (0.35)	37.59 (0.39)	37.94 (0.41)	38.22 (0.42)	38.45 (0.44)
Yeongcheon	35.79 (0.36)	36.62 (0.41)	37.44 (0.44)	37.92 (0.46)	38.31 (0.45)	38.64 (0.43)
Geochang	35.04 (0.33)	35.79 (0.37)	36.54 (0.40)	36.98 (0.41)	37.34 (0.40)	37.63 (0.38)
Hapcheon	36.43 (0.40)	37.33 (0.47)	38.22 (0.54)	38.74 (0.56)	39.17 (0.57)	39.52 (0.57)
Miryang	36.58 (0.39)	37.47 (0.46)	38.35 (0.51)	38.86 (0.54)	39.29 (0.54)	39.63 (0.53)
Sancheong	35.97 (0.37)	36.83 (0.44)	37.69 (0.49)	38.19 (0.51)	38.60 (0.52)	38.94 (0.51)
Geoje	31.83 (0.57)	32.83 (0.64)	33.81 (0.69)	34.39 (0.72)	34.87 (0.73)	35.26 (0.72)
Namhae	32.26 (0.55)	33.25 (0.61)	34.24 (0.67)	34.82 (0.69)	35.29 (0.70)	35.68 (0.69)

Table 9: Geographic information (latitude, longitude, altitude, distance to coast, and geographic region) for 108 unobserved locations and predicted parameters with standard errors in parenthesis from 4 regional models via max-stable processes. For the location near the boundaries of the four regions, we obtained two values from the two regional models for adjacent regions (unit: degree Celsius).

Location	Latit.	longit.	altit.	coast	region	location		scale		shape	
Seongnam si	37.26	127.09	84	5	NW	33.99	(0.20)	1.36	(0.11)	-0.24	(0.05)
Uijeongbu si	37.44	127.02	89	5	NW	33.96	(0.20)	1.36	(0.11)	-0.24	(0.05)
Anyang si	37.23	126.58	12	1	NW	33.06	(0.24)	1.50	(0.13)	-0.24	(0.05)
Bucheon si	37.28	126.46	48	1	NW	32.84	(0.24)	1.50	(0.13)	-0.24	(0.05)
Gwangmyeong si	37.26	126.50	5	1	NW	33.10	(0.24)	1.50	(0.13)	-0.24	(0.05)
Pyeongtaek si	36.59	127.06	286	6	NW	33.72	(0.21)	1.22	(0.11)	-0.24	(0.05)
Dongducheon si	37.54	127.03	9	5	NW	34.44	(0.21)	1.36	(0.11)	-0.24	(0.05)
Ansan si	37.23	126.46	0	1	NW	33.13	(0.24)	1.50	(0.13)	-0.24	(0.05)
Goyangsi	37.36	126.51	0	1	NW	33.13	(0.24)	1.50	(0.13)	-0.24	(0.05)
Gwacheon si	37.26	126.59	51	1	NW	32.82	(0.24)	1.50	(0.13)	-0.24	(0.05)
Guri si	37.36	127.08	120	5	NW	33.77	(0.20)	1.36	(0.11)	-0.24	(0.05)
Namyangju si	37.38	127.12	53	5	NW	34.18	(0.21)	1.36	(0.11)	-0.24	(0.05)
Osan si	37.09	127.05	14	5	NW	34.41	(0.21)	1.36	(0.11)	-0.24	(0.05)
Siheung si	37.24	126.47	4	1	NW	33.11	(0.24)	1.50	(0.13)	-0.24	(0.05)
Gunpo si	37.21	126.57	31	1	NW	32.94	(0.24)	1.50	(0.13)	-0.24	(0.05)
Uiwang si	37.20	126.57	11	1	NW	33.06	(0.24)	1.50	(0.13)	-0.24	(0.05)
Hanam si	37.32	127.12	109	5	NW	33.84	(0.20)	1.36	(0.11)	-0.24	(0.05)
Yongin si	37.14	127.11	100	5	NW	33.89	(0.20)	1.36	(0.11)	-0.24	(0.05)
Paju si	37.45	126.46	5	1	NW	33.10	(0.24)	1.50	(0.13)	-0.24	(0.05)
Anseong si	37.00	127.16	22	5	NW	34.36	(0.21)	1.36	(0.11)	-0.24	(0.05)
Gimpo si	37.37	126.43	63	1	NW	32.75	(0.24)	1.50	(0.13)	-0.24	(0.05)
Hwaseong si	37.06	126.50	1	1	NW	33.12	(0.24)	1.50	(0.13)	-0.24	(0.05)
Gwangju si	37.25	127.16	213	6	NW	33.55	(0.21)	1.32	(0.11)	-0.24	(0.05)
Yangju gun	37.47	127.02	66	5	NW	34.10	(0.21)	1.36	(0.11)	-0.24	(0.05)
Pocheon si	37.53	127.13	32	5	NW	34.30	(0.21)	1.36	(0.11)	-0.24	(0.05)
Yeoju gun	37.57	127.00	24	5	NW	34.35	(0.21)	1.36	(0.11)	-0.24	(0.05)
Yeoncheon gun	38.05	127.04	80	5	NW	34.83	(0.28)	1.46	(0.13)	-0.24	(0.05)
Gapyeong gun	37.49	127.30	78	5	NW	34.02	(0.20)	1.36	(0.11)	-0.24	(0.05)
Donghae si	37.32	129.06	401	4	NE	33.21	(0.27)	1.39	(0.10)	-0.30	(0.05)
Taebaek si	37.06	128.59	756	6	NE	31.34	(0.54)	1.29	(0.10)	-0.30	(0.05)
Samcheok si	37.27	129.10	531	4	NE	32.47	(0.37)	1.39	(0.10)	-0.30	(0.05)
Hoengseong gun	37.29	127.60	83	5	NE	35.16	(0.22)	1.34	(0.10)	-0.30	(0.05)
					NW	33.99	(0.20)	1.36	(0.11)	-0.24	(0.05)
Yeongwol gun	37.11	128.27	271	6	NE	34.10	(0.20)	1.29	(0.10)	-0.30	(0.05)
Pyeongchang gun	37.22	128.23	374	6	NE	33.51	(0.24)	1.29	(0.10)	-0.30	(0.05)

Table 10: Table 9 continued

Location	Latit.	longit.	altit.	coast	region	location	scale	shape
Jeongseon gun	37.22	128.39	287	6	NE	34.00 (0.20)	1.29 (0.10)	-0.30 (0.05)
Cheorwon gun	38.09	127.18	449	6	NE	32.55 (0.32)	1.29 (0.10)	-0.30 (0.05)
Hwacheon gun	38.06	127.43	551	6	NE	31.97 (0.40)	1.29 (0.10)	-0.30 (0.05)
					NW	32.32 (0.29)	1.43 (0.13)	-0.24 (0.05)
Yanggu gun	38.06	127.59	467	6	NE	32.45 (0.33)	1.29 (0.10)	-0.30 (0.05)
					NW	32.83 (0.27)	1.43 (0.13)	-0.24 (0.05)
Goseong gun	38.22	128.28	1023	6	NE	29.26 (0.77)	1.29 (0.10)	-0.30 (0.05)
Yangyang gun	38.05	128.37	768	6	NE	30.71 (0.55)	1.29 (0.10)	-0.30 (0.05)
Cheongwon gun	36.33	127.32	49	5	NW	34.81 (0.21)	1.25 (0.11)	-0.24 (0.05)
Okcheon gun	36.18	127.34	304	6	NW	33.61 (0.21)	1.22 (0.11)	-0.24 (0.05)
					NE	33.32 (0.35)	1.29 (0.10)	-0.30 (0.05)
Yeongdong gun	36.11	127.48	178	5	NW	34.03 (0.21)	1.25 (0.11)	-0.24 (0.05)
					NE	33.99 (0.30)	1.34 (0.10)	-0.30 (0.05)
Jeungpyeong gun	36.47	127.35	50	5	NW	34.80 (0.21)	1.25 (0.11)	-0.24 (0.05)
					NE	34.72 (0.25)	1.34 (0.10)	-0.30 (0.05)
Jincheon gun	36.51	127.26	29	5	NW	34.93 (0.21)	1.25 (0.11)	-0.24 (0.05)
Goesan gun	36.48	127.47	208	6	NE	33.87 (0.29)	1.29 (0.10)	-0.30 (0.05)
					NW	34.19 (0.20)	1.22 (0.11)	-0.24 (0.05)
Eumseong gun	36.56	127.42	189	5	NW	33.96 (0.21)	1.25 (0.11)	-0.24 (0.05)
					NE	33.93 (0.31)	1.34 (0.10)	-0.30 (0.05)
Danyang gun	36.59	128.22	65	5	NW	34.71 (0.21)	1.25 (0.11)	-0.24 (0.05)
Gongju si	36.27	127.07	6	5	NW	35.07 (0.21)	1.25 (0.11)	-0.24 (0.05)
Asan si	36.47	127.00	145	5	NW	34.23 (0.20)	1.25 (0.11)	-0.24 (0.05)
Nonsan si	36.11	127.06	6	5	NW	35.07 (0.21)	1.25 (0.11)	-0.24 (0.05)
Gyeryong si	36.17	127.15	21	5	NW	34.98 (0.21)	1.25 (0.11)	-0.24 (0.05)
Dangjin gun	36.53	126.38	13	1	NW	33.66 (0.24)	1.40 (0.12)	-0.24 (0.05)
Yeongi gun	36.35	127.17	131	5	NW	34.31 (0.20)	1.25 (0.11)	-0.24 (0.05)
Seocheon gun	36.08	126.44	0	1	NW	33.74 (0.25)	1.40 (0.12)	-0.24 (0.05)
Cheongyang gun	36.30	126.52	0	1	NW	33.74 (0.25)	1.40 (0.12)	-0.24 (0.05)
Hongseong gun	36.37	126.40	37	1	NW	33.52 (0.24)	1.40 (0.12)	-0.24 (0.05)
Yesan gun	36.40	126.50	31	1	NW	33.55 (0.24)	1.40 (0.12)	-0.24 (0.05)
Taean gun	36.45	126.31	0	1	NW	33.74 (0.25)	1.40 (0.12)	-0.24 (0.05)
Dangjin si	36.57	126.33	26	1	NW	33.58 (0.24)	1.40 (0.12)	-0.24 (0.05)
Iksan si	35.59	126.57	15	1	SW	33.03 (0.26)	1.57 (0.12)	-0.27 (0.06)
Gimje si	35.48	126.53	13	1	SW	33.05 (0.26)	1.57 (0.12)	-0.27 (0.06)
Wanju gun	35.53	127.15	223	6	SW	33.19 (0.27)	1.57 (0.12)	-0.27 (0.06)
Jinan gun	35.47	127.25	150	5	SW	33.76 (0.26)	1.57 (0.12)	-0.27 (0.06)
Muju gun	36.01	127.39	477	6	SW	30.84 (0.28)	1.26 (0.09)	-0.27 (0.06)
					SE	33.80 (0.26)	1.24 (0.16)	-0.28 (0.05)
Jangsu gun	35.38	127.31	83	5	SW	34.27 (0.26)	1.57 (0.12)	-0.27 (0.06)
Sunchang gun	35.22	127.09	240	6	SW	33.06 (0.27)	1.57 (0.12)	-0.27 (0.06)
Gochang gun	35.26	126.43	4	1	SW	33.12 (0.26)	1.57 (0.12)	-0.27 (0.06)
Naju si	35.00	126.42	10	1	SW	33.07 (0.26)	1.57 (0.12)	-0.27 (0.06)
Gwangyang si	34.56	127.41	40	1	SE	29.55 (0.47)	2.20 (0.26)	-0.28 (0.05)
					SW	31.54 (0.36)	1.89 (0.16)	-0.27 (0.06)

Table 11: Table 9 continued

Location	Latit.	longit.	altit.	coast	region	location	scale		shape	
Damyang gun	35.20	126.59	53	3	SW	32.74 (0.27)	1.57	(0.12)	-0.27	(0.06)
Gokseong gun	35.16	127.17	511	6	SW	30.97 (0.33)	1.57	(0.12)	-0.27	(0.06)
Gurye gun	35.12	127.27	48	5	SW	34.54 (0.26)	1.57	(0.12)	-0.27	(0.06)
Boseong gun	34.45	127.04	115	1	SW	30.96 (0.36)	1.89	(0.16)	-0.27	(0.06)
Hwasun gun	35.04	126.59	5	3	SW	33.11 (0.26)	1.57	(0.12)	-0.27	(0.06)
Gangjin gun	34.38	126.49	25	1	SW	29.89 (0.36)	1.89	(0.16)	-0.27	(0.06)
Yeongam gun	34.49	126.38	42	1	SW	29.76 (0.36)	1.89	(0.16)	-0.27	(0.06)
Muan gun	34.60	126.29	5	1	SW	30.04 (0.36)	1.89	(0.16)	-0.27	(0.06)
Hampyeong gun	35.05	126.30	5	1	SW	33.11 (0.26)	1.57	(0.12)	-0.27	(0.06)
Yeonggwang gun	35.19	126.30	0	1	SW	33.15 (0.27)	1.57	(0.12)	-0.27	(0.06)
Jangseong gun	35.18	126.47	103	1	SW	32.35 (0.27)	1.57	(0.12)	-0.27	(0.06)
Jindo gun	34.25	126.18	38	1	SW	29.79 (0.36)	1.89	(0.16)	-0.27	(0.06)
Sinan gun	34.49	126.06	28	1	SW	29.86 (0.36)	1.89	(0.16)	-0.27	(0.06)
Gyeongju si	35.51	129.14	127	3	SE	32.47 (0.27)	1.79	(0.18)	-0.28	(0.05)
Gimcheon si	36.09	128.06	308	6	NE	33.26 (0.32)	1.29	(0.10)	-0.30	(0.05)
Andong si	36.34	128.44	48	5	NE	34.70 (0.22)	1.34	(0.10)	-0.30	(0.05)
Sangju si	36.24	128.09	146	5	NE	34.14 (0.25)	1.34	(0.10)	-0.30	(0.05)
Gyeongsan si	35.49	128.44	25	5	SE	34.03 (0.28)	1.94	(0.21)	-0.28	(0.05)
Gunwi gun	36.14	128.34	113	5	NE	34.33 (0.24)	1.34	(0.10)	-0.30	(0.05)
Cheongsong gun	36.26	129.04	292	6	NE	33.29 (0.26)	1.29	(0.10)	-0.30	(0.05)
Yeongyang gun	36.39	129.07	193	5	NE	33.81 (0.22)	1.34	(0.10)	-0.30	(0.05)
Cheongdo gun	35.39	128.44	3	5	SE	34.20 (0.29)	1.96	(0.22)	-0.28	(0.05)
Goryeong gun	35.43	128.16	179	5	SE	32.87 (0.27)	1.83	(0.20)	-0.28	(0.05)
Seongju gun	35.55	128.16	102	5	SE	33.45 (0.27)	1.89	(0.21)	-0.28	(0.05)
Chilgok gun	35.59	128.24	177	5	SE	32.89 (0.27)	1.83	(0.20)	-0.28	(0.05)
Yecheon gun	36.40	128.27	76	5	NE	34.54 (0.23)	1.34	(0.10)	-0.30	(0.05)
Bonghwa gun	36.53	128.43	55	5	NE	34.66 (0.22)	1.34	(0.10)	-0.30	(0.05)
Ulleung gun	37.49	130.80	67	1	NE	34.89 (0.24)	1.54	(0.12)	-0.30	(0.05)
Changwon si	35.16	128.39	345	2	NE	31.08 (0.80)	1.49	(0.11)	-0.30	(0.05)
Sacheon si	35.00	128.04	5	1	SE	34.18 (0.29)	1.81	(0.17)	-0.28	(0.05)
Gimhae si	35.14	128.53	163	1	SE	32.99 (0.27)	1.69	(0.17)	-0.28	(0.05)
Yangsan si	35.20	129.02	452	2	SE	30.02 (0.34)	1.53	(0.21)	-0.28	(0.05)
Uiryeong gun	35.19	128.15	28	3	SE	34.01 (0.28)	1.87	(0.19)	-0.28	(0.05)
Haman gun	35.16	128.24	79	3	SE	33.62 (0.27)	1.83	(0.18)	-0.28	(0.05)
Changnyeong gun	35.33	128.29	9	5	SE	34.15 (0.29)	1.95	(0.22)	-0.28	(0.05)
Goseong gun	34.57	128.18	0	1	SE	29.43 (0.47)	2.23	(0.27)	-0.28	(0.05)
Hadong gun	35.04	127.45	263	4	SE	32.66 (0.27)	1.74	(0.19)	-0.28	(0.05)
					SW	32.88 (0.27)	1.57	(0.12)	-0.27	(0.06)
Hamyang gun	35.32	127.44	121	5	SE	33.73 (0.29)	1.87	(0.20)	-0.28	(0.05)
					SW	33.98 (0.26)	1.57	(0.12)	-0.27	(0.06)

Table 12: Return levels for several return periods (standard errors in parenthesis) for 108 unobserved locations, calculated using the estimates of $\hat{\mu}(x_0)$, $\hat{\sigma}(x_0)$, $\hat{\xi}(x_0)$ from the max-stable processes regional models. For the location near the boundaries of the four regions, we obtained two values from the two regional models for adjacent regions (unit: degree Celsius).

Location	5 year	10 year	25 year	50 year	100 year	200 year
Seongnam si	35.70 (0.29)	36.35 (0.34)	37.01 (0.42)	37.42 (0.49)	37.76 (0.55)	38.05 (0.61)
Uijeongbu si	35.67 (0.29)	36.32 (0.34)	36.98 (0.42)	37.39 (0.49)	37.73 (0.55)	38.02 (0.61)
Anyang si	34.95 (0.32)	35.67 (0.38)	36.41 (0.47)	36.86 (0.54)	37.23 (0.61)	37.55 (0.68)
Bucheon si	34.73 (0.32)	35.45 (0.38)	36.19 (0.47)	36.64 (0.54)	37.01 (0.61)	37.33 (0.68)
Gwangmyeong si	34.99 (0.32)	35.71 (0.38)	36.45 (0.47)	36.90 (0.54)	37.27 (0.61)	37.59 (0.68)
Pyeongtaek si	35.25 (0.28)	35.83 (0.33)	36.43 (0.40)	36.79 (0.45)	37.09 (0.51)	37.35 (0.56)
Dongducheon si	36.15 (0.29)	36.80 (0.35)	37.47 (0.42)	37.87 (0.49)	38.21 (0.55)	38.50 (0.61)
Ansan si	35.02 (0.32)	35.74 (0.38)	36.48 (0.47)	36.93 (0.54)	37.30 (0.61)	37.62 (0.68)
Goyangsi	35.02 (0.32)	35.74 (0.38)	36.48 (0.47)	36.93 (0.54)	37.30 (0.61)	37.62 (0.68)
Gwacheon si	34.71 (0.32)	35.43 (0.38)	36.17 (0.47)	36.62 (0.54)	37.00 (0.61)	37.31 (0.68)
Guri si	35.48 (0.29)	36.13 (0.34)	36.80 (0.42)	37.20 (0.49)	37.54 (0.55)	37.83 (0.61)
Namyangju si	35.88 (0.29)	36.53 (0.34)	37.20 (0.42)	37.61 (0.49)	37.95 (0.55)	38.23 (0.61)
Osan si	36.12 (0.29)	36.77 (0.35)	37.44 (0.42)	37.84 (0.49)	38.18 (0.55)	38.47 (0.61)
Siheung si	35.00 (0.32)	35.71 (0.38)	36.45 (0.47)	36.90 (0.54)	37.28 (0.61)	37.60 (0.68)
Gunpo si	34.83 (0.32)	35.55 (0.38)	36.29 (0.47)	36.74 (0.54)	37.12 (0.61)	37.43 (0.68)
Uiwang si	34.95 (0.32)	35.67 (0.38)	36.41 (0.47)	36.86 (0.54)	37.24 (0.61)	37.56 (0.68)
Hanam si	35.55 (0.29)	36.19 (0.34)	36.86 (0.42)	37.27 (0.49)	37.61 (0.55)	37.90 (0.61)
Yongin si	35.60 (0.29)	36.25 (0.34)	36.92 (0.42)	37.32 (0.49)	37.66 (0.55)	37.95 (0.61)
Paju si	34.99 (0.32)	35.71 (0.38)	36.45 (0.47)	36.90 (0.54)	37.27 (0.61)	37.59 (0.68)
Anseong si	36.07 (0.29)	36.72 (0.35)	37.39 (0.42)	37.79 (0.49)	38.13 (0.55)	38.42 (0.61)
Gimpo si	34.64 (0.32)	35.36 (0.38)	36.10 (0.47)	36.55 (0.54)	36.92 (0.61)	37.24 (0.68)
Hwaseong si	35.01 (0.32)	35.73 (0.38)	36.47 (0.47)	36.92 (0.54)	37.30 (0.61)	37.62 (0.68)
Gwangju si	35.21 (0.28)	35.84 (0.34)	36.49 (0.41)	36.89 (0.48)	37.22 (0.54)	37.50 (0.60)
Yangju gun	35.81 (0.29)	36.45 (0.34)	37.12 (0.42)	37.53 (0.49)	37.87 (0.55)	38.16 (0.61)
Pocheon si	36.01 (0.29)	36.66 (0.34)	37.33 (0.42)	37.73 (0.49)	38.07 (0.55)	38.36 (0.61)
Yeoju gun	36.06 (0.29)	36.71 (0.35)	37.38 (0.42)	37.78 (0.49)	38.12 (0.55)	38.41 (0.61)
Yeoncheon gun	36.67 (0.35)	37.37 (0.40)	38.09 (0.48)	38.53 (0.55)	38.89 (0.61)	39.20 (0.68)
Gapyeong gun	35.73 (0.29)	36.38 (0.34)	37.05 (0.42)	37.46 (0.49)	37.80 (0.55)	38.08 (0.61)
Donghae si	34.89 (0.33)	35.49 (0.36)	36.07 (0.39)	36.41 (0.41)	36.69 (0.42)	36.91 (0.44)
Taebaek si	32.90 (0.59)	33.45 (0.61)	34.00 (0.64)	34.31 (0.65)	34.57 (0.67)	34.77 (0.68)
Samcheok si	34.15 (0.42)	34.75 (0.45)	35.34 (0.48)	35.67 (0.49)	35.95 (0.51)	36.17 (0.52)
Hoengseong gun	36.78 (0.27)	37.35 (0.30)	37.92 (0.33)	38.25 (0.35)	38.51 (0.36)	38.72 (0.38)
	35.70 (0.29)	36.35 (0.34)	37.02 (0.42)	37.43 (0.49)	37.77 (0.55)	38.05 (0.61)
Yeongwol gun	35.66 (0.25)	36.21 (0.28)	36.76 (0.31)	37.07 (0.33)	37.32 (0.35)	37.53 (0.36)
Pyeongchang gun	35.07 (0.30)	35.63 (0.33)	36.17 (0.36)	36.49 (0.38)	36.74 (0.40)	36.94 (0.41)
Jeongseon gun	35.57 (0.26)	36.12 (0.29)	36.67 (0.32)	36.98 (0.34)	37.23 (0.36)	37.44 (0.37)
Cheorwon gun	34.12 (0.37)	34.67 (0.40)	35.22 (0.42)	35.53 (0.44)	35.78 (0.45)	35.99 (0.47)
Hwacheon gun	33.54 (0.45)	34.09 (0.47)	34.64 (0.50)	34.95 (0.51)	35.20 (0.53)	35.41 (0.54)
	34.12 (0.35)	34.80 (0.41)	35.50 (0.48)	35.93 (0.55)	36.29 (0.61)	36.59 (0.67)

Table 13: Table 12 continued

Location	5 year	10 year	25 year	50 year	100 year	200 year
Yanggu gun	34.02 (0.38)	34.57 (0.41)	35.11 (0.44)	35.43 (0.45)	35.68 (0.47)	35.89 (0.48)
	34.63 (0.34)	35.31 (0.40)	36.01 (0.48)	36.44 (0.54)	36.80 (0.60)	37.10 (0.67)
Goseong gun	30.82 (0.81)	31.37 (0.83)	31.92 (0.85)	32.23 (0.87)	32.49 (0.88)	32.69 (0.88)
Yangyang gun	32.27 (0.59)	32.82 (0.61)	33.37 (0.63)	33.68 (0.65)	33.94 (0.66)	34.14 (0.67)
Cheongwon gun	36.38 (0.28)	36.98 (0.33)	37.60 (0.40)	37.97 (0.46)	38.29 (0.52)	38.55 (0.58)
Okcheon gun	35.14 (0.28)	35.72 (0.33)	36.32 (0.40)	36.68 (0.45)	36.99 (0.51)	37.24 (0.56)
	34.88 (0.40)	35.44 (0.43)	35.98 (0.45)	36.30 (0.47)	36.55 (0.49)	36.75 (0.50)
Yeongdong gun	35.60 (0.28)	36.20 (0.33)	36.82 (0.40)	37.19 (0.46)	37.51 (0.52)	37.77 (0.57)
	35.62 (0.36)	36.19 (0.39)	36.76 (0.42)	37.08 (0.44)	37.35 (0.45)	37.56 (0.46)
Jeungpyeong gun	36.38 (0.28)	36.98 (0.33)	37.59 (0.40)	37.97 (0.46)	38.28 (0.52)	38.54 (0.58)
	36.34 (0.31)	36.92 (0.33)	37.49 (0.36)	37.81 (0.38)	38.08 (0.40)	38.29 (0.41)
Jincheon gun	36.51 (0.28)	37.10 (0.33)	37.72 (0.41)	38.09 (0.46)	38.41 (0.52)	38.67 (0.58)
Goesan gun	35.43 (0.34)	35.98 (0.37)	36.53 (0.40)	36.84 (0.42)	37.10 (0.43)	37.30 (0.44)
	35.72 (0.27)	36.30 (0.32)	36.90 (0.39)	37.26 (0.45)	37.57 (0.51)	37.82 (0.56)
Eumseong gun	35.54 (0.28)	36.14 (0.33)	36.75 (0.40)	37.13 (0.46)	37.44 (0.52)	37.70 (0.57)
	35.55 (0.37)	36.13 (0.39)	36.70 (0.42)	37.02 (0.44)	37.28 (0.46)	37.50 (0.47)
Danyang gun	36.29 (0.28)	36.89 (0.33)	37.50 (0.40)	37.88 (0.46)	38.19 (0.52)	38.45 (0.58)
Gongju si	36.64 (0.29)	37.24 (0.34)	37.86 (0.41)	38.23 (0.46)	38.55 (0.52)	38.81 (0.58)
Asan si	35.80 (0.28)	36.40 (0.33)	37.02 (0.40)	37.39 (0.46)	37.71 (0.52)	37.97 (0.57)
Nonsan si	36.64 (0.29)	37.24 (0.34)	37.86 (0.41)	38.23 (0.46)	38.55 (0.52)	38.81 (0.58)
Gyeryong si	36.55 (0.28)	37.15 (0.33)	37.77 (0.41)	38.14 (0.46)	38.46 (0.52)	38.72 (0.58)
Dangjin gun	35.42 (0.32)	36.09 (0.37)	36.77 (0.45)	37.19 (0.51)	37.54 (0.57)	37.84 (0.64)
Yeongi gun	35.50 (0.32)	36.16 (0.37)	36.85 (0.45)	37.27 (0.51)	37.62 (0.57)	37.91 (0.64)
Seocheon gun	35.50 (0.32)	36.16 (0.37)	36.85 (0.45)	37.27 (0.51)	37.62 (0.57)	37.91 (0.64)
Cheongyang gun	35.27 (0.31)	35.94 (0.37)	36.63 (0.45)	37.05 (0.51)	37.40 (0.57)	37.69 (0.64)
Hongseong gun	35.31 (0.31)	35.98 (0.37)	36.67 (0.45)	37.08 (0.51)	37.43 (0.57)	37.73 (0.64)
Yesan gun	35.50 (0.32)	36.16 (0.37)	36.85 (0.45)	37.27 (0.51)	37.62 (0.57)	37.91 (0.64)
Taean gun	35.34 (0.31)	36.01 (0.37)	36.70 (0.45)	37.11 (0.51)	37.46 (0.57)	37.76 (0.64)
Dangjin si	34.98 (0.33)	35.69 (0.36)	36.42 (0.39)	36.84 (0.39)	37.20 (0.39)	37.49 (0.38)
Iksan si	34.99 (0.33)	35.71 (0.36)	36.43 (0.39)	36.86 (0.39)	37.21 (0.39)	37.50 (0.38)
Gimje si	35.14 (0.34)	35.85 (0.37)	36.58 (0.39)	37.00 (0.40)	37.36 (0.40)	37.65 (0.39)
Wanju gun	35.70 (0.33)	36.42 (0.36)	37.14 (0.39)	37.57 (0.40)	37.92 (0.39)	38.21 (0.38)
Jinan gun	32.40 (0.33)	32.98 (0.35)	33.55 (0.36)	33.90 (0.37)	34.18 (0.37)	34.41 (0.36)
Muji gun	36.22 (0.33)	36.93 (0.36)	37.66 (0.39)	38.08 (0.40)	38.44 (0.40)	38.73 (0.39)
	35.32 (0.33)	35.87 (0.37)	36.42 (0.41)	36.74 (0.43)	37.00 (0.44)	37.22 (0.44)
Jangsu gun	35.01 (0.34)	35.72 (0.37)	36.44 (0.39)	36.87 (0.40)	37.23 (0.40)	37.52 (0.39)
Sunchang gun	35.06 (0.33)	35.78 (0.36)	36.50 (0.39)	36.93 (0.39)	37.28 (0.39)	37.57 (0.38)
Gochang gun	35.02 (0.33)	35.73 (0.36)	36.45 (0.39)	36.88 (0.39)	37.24 (0.39)	37.53 (0.38)
Naju si	32.24 (0.54)	33.21 (0.59)	34.19 (0.64)	34.76 (0.66)	35.23 (0.66)	35.61 (0.65)
Gwangyang si	34.68 (0.33)	35.40 (0.36)	36.12 (0.39)	36.55 (0.39)	36.90 (0.39)	37.19 (0.38)
	33.87 (0.44)	34.73 (0.49)	35.59 (0.52)	36.11 (0.53)	36.53 (0.54)	36.88 (0.53)
Damyang gun	32.91 (0.38)	33.63 (0.41)	34.35 (0.43)	34.78 (0.44)	35.13 (0.43)	35.43 (0.42)
Gokseong gun	36.49 (0.33)	37.20 (0.37)	37.93 (0.39)	38.35 (0.40)	38.71 (0.40)	39.00 (0.39)
Gurye gun	33.29 (0.45)	34.15 (0.49)	35.01 (0.52)	35.53 (0.53)	35.95 (0.54)	36.30 (0.53)

Table 14: Table 12 continued

Location	5 year	10 year	25 year	50 year	100 year	200 year
Boseong gun	35.05 (0.33)	35.77 (0.36)	36.49 (0.39)	36.92 (0.39)	37.27 (0.39)	37.57 (0.38)
Hwasun gun	32.22 (0.44)	33.08 (0.48)	33.94 (0.51)	34.46 (0.52)	34.88 (0.53)	35.23 (0.52)
Gangjin gun	32.09 (0.44)	32.95 (0.48)	33.81 (0.51)	34.33 (0.53)	34.75 (0.53)	35.10 (0.52)
Yeongam gun	32.37 (0.44)	33.23 (0.48)	34.10 (0.51)	34.61 (0.52)	35.03 (0.53)	35.38 (0.52)
Muan gun	35.05 (0.33)	35.77 (0.36)	36.49 (0.39)	36.92 (0.39)	37.27 (0.39)	37.57 (0.38)
Hampyeong gun	35.09 (0.33)	35.81 (0.36)	36.53 (0.39)	36.96 (0.39)	37.31 (0.39)	37.60 (0.38)
Yeonggwang gun	34.30 (0.33)	35.01 (0.36)	35.74 (0.39)	36.16 (0.39)	36.52 (0.39)	36.81 (0.38)
Jangseong gun	32.12 (0.44)	32.98 (0.48)	33.84 (0.51)	34.36 (0.53)	34.78 (0.53)	35.13 (0.52)
Jindo gun	32.20 (0.44)	33.06 (0.48)	33.92 (0.51)	34.43 (0.53)	34.86 (0.53)	35.21 (0.52)
Sinan gun	34.67 (0.36)	35.47 (0.41)	36.26 (0.45)	36.73 (0.46)	37.11 (0.45)	37.42 (0.43)
Gyeongju si	34.83 (0.36)	35.38 (0.39)	35.93 (0.42)	36.24 (0.43)	36.49 (0.45)	36.70 (0.46)
Gimcheon si	36.32 (0.27)	36.90 (0.30)	37.46 (0.33)	37.79 (0.34)	38.05 (0.36)	38.27 (0.37)
Andong si	35.25 (0.32)	35.80 (0.34)	36.35 (0.37)	36.66 (0.39)	36.91 (0.40)	37.12 (0.42)
Sangju si	35.77 (0.30)	36.34 (0.33)	36.91 (0.36)	37.23 (0.38)	37.50 (0.40)	37.71 (0.41)
Gyeongsan si	36.41 (0.38)	37.27 (0.44)	38.13 (0.48)	38.64 (0.50)	39.05 (0.50)	39.39 (0.49)
Gunwi gun	35.95 (0.29)	36.53 (0.32)	37.09 (0.35)	37.42 (0.37)	37.68 (0.38)	37.90 (0.40)
Cheongsong gun	34.86 (0.29)	35.41 (0.32)	35.95 (0.34)	36.27 (0.36)	36.52 (0.37)	36.73 (0.39)
Yeongyang gun	35.44 (0.27)	36.01 (0.29)	36.58 (0.32)	36.90 (0.34)	37.17 (0.36)	37.38 (0.37)
Cheongdo gun	36.59 (0.38)	37.46 (0.44)	38.33 (0.49)	38.84 (0.51)	39.26 (0.51)	39.60 (0.50)
Goryeong gun	35.11 (0.36)	35.93 (0.41)	36.74 (0.46)	37.22 (0.47)	37.61 (0.47)	37.92 (0.46)
Seongju gun	35.76 (0.37)	36.60 (0.42)	37.44 (0.47)	37.93 (0.48)	38.33 (0.48)	38.66 (0.47)
Chilgok gun	35.13 (0.36)	35.95 (0.41)	36.76 (0.46)	37.24 (0.47)	37.62 (0.47)	37.94 (0.46)
Yecheon gun	36.16 (0.28)	36.74 (0.30)	37.31 (0.33)	37.63 (0.35)	37.89 (0.37)	38.11 (0.38)
Bonghwa gun	36.28 (0.27)	36.86 (0.30)	37.42 (0.33)	37.75 (0.35)	38.01 (0.36)	38.23 (0.38)
Ulleung gun	36.75 (0.26)	37.41 (0.28)	38.06 (0.31)	38.44 (0.33)	38.74 (0.35)	38.98 (0.36)
Changwon si	32.88 (0.84)	33.52 (0.87)	34.15 (0.89)	34.51 (0.90)	34.81 (0.91)	35.04 (0.92)
Sacheon si	36.39 (0.34)	37.20 (0.38)	38.00 (0.41)	38.47 (0.41)	38.85 (0.40)	39.16 (0.37)
Gimhae si	35.07 (0.33)	35.82 (0.37)	36.57 (0.40)	37.01 (0.40)	37.37 (0.39)	37.66 (0.37)
Yangsan si	31.89 (0.43)	32.57 (0.48)	33.24 (0.53)	33.64 (0.55)	33.96 (0.57)	34.23 (0.57)
Uiryeong gun	36.29 (0.35)	37.12 (0.40)	37.95 (0.44)	38.43 (0.44)	38.83 (0.44)	39.15 (0.42)
Haman gun	35.86 (0.35)	36.68 (0.39)	37.49 (0.43)	37.96 (0.43)	38.35 (0.43)	38.67 (0.41)
Changnyeong gun	36.54 (0.38)	37.41 (0.44)	38.28 (0.49)	38.78 (0.50)	39.20 (0.51)	39.54 (0.49)
Goseong gun	32.16 (0.56)	33.15 (0.62)	34.13 (0.67)	34.71 (0.69)	35.18 (0.70)	35.57 (0.69)
Hadong gun	34.78 (0.34)	35.55 (0.38)	36.32 (0.42)	36.77 (0.43)	37.14 (0.43)	37.44 (0.42)
	34.83 (0.34)	35.54 (0.37)	36.27 (0.39)	36.70 (0.40)	37.05 (0.40)	37.34 (0.39)
Hamyang gun	36.02 (0.35)	36.85 (0.40)	37.68 (0.45)	38.17 (0.46)	38.57 (0.45)	38.89 (0.44)
	35.92 (0.33)	36.64 (0.36)	37.36 (0.39)	37.79 (0.40)	38.14 (0.39)	38.43 (0.39)